PERIODICO di MINERALOGIA
established in 1930

DIPARTIMENTO
DI SCIENZE DELLA TERRA
SAPIENZA
UNIVERSITÀ DI ROMA

An International Journal of
Mineralogy, Crystallography, Geochemistry,
Ore Deposits, Petrology, Volcanology
and applied topics on Environment, Archaeometry and Cultural Heritage

A Windows program for pyroxene-liquid thermobarometry

Fuat Yavuz* and Demet Kıran Yıldırım

Department of Geological Engineering, Istanbul Technical University, 34469 Maslak, Istanbul, Turkey

ARTICLE INFO

Submitted: April 2018
Accepted: May 2018
Available on line: June 2018

* Corresponding author:
yavuz@itu.edu.tr

DOI: 10.2451/2018PM787

How to cite this article:
Yavuz F. et al. (2018)
Period. Mineral. 87, 149-172

ABSTRACT

A Windows program (WinPLtb) has been developed to calculate wet-chemical and microprobe pyroxene analyses based on the standard International Mineralogical Association (IMA-88) nomenclature scheme. The program allows the user to enter clinopyroxene, orthopyroxene and associated composition of liquid or whole-rock and some calculated components in the *Data Entry Screen* as well as loading the Microsoft® Excel files including pyroxene and liquid analyses. Although, WinPLtb is essentially aimed to estimate the clinopyroxene-liquid and orthopyrpxene-liquid thermobarometers it also calculates the clinopyroxene-based hygrometers and depths where pyroxene-bearing rocks crystallized. Calculation of pressure- and temperature-dependent thermobarometers is carried out using the previously entered input *P*-*T* values or calculated *P*-*T* values by program depending on the selected options from pull-down menu. The input values for calculations are percentage of clinopyroxene and orthopyroxene analyses, liquid or whole-rock compositions, *P* (GPa) for temperature-dependent orthopyroxene-liquid thermometers, and *T* (K)-*P* (kbar) for clinopyroxene-liquid thermobarometers. All the calculated results by program are stored in an output Excel file. This file can be used for further general data manipulation and graphing purposes. The compiled program described herein is distributed as a self-extracting setup file, including the necessary support files used by program, a help file, and sample data files.

Keywords: Pyroxene; liquid; classification; thermometer; barometer, hygrometer, depth; software.

INTRODUCTION

The study of earth materials from physicochemical point of view has attracted attention of geologists to estimate the pressure *(P)* and temperature *(T)* conditions of igneous and metamorphic rocks. Although early approaches were mostly qualitative, the later studies which are based on an experimental petrology allowed more quantitative evaluations to addressing the conditions of magmatic and metamorphic processes (Winter, 2001). The *P*-*T* studies, thus played an important role in igneous and metamorphic petrology as they provide critical evidence in understanding of the tectonic, thermal structure, and history of Earth's upper mantle compositions.

Because of its ubiquity in igneous and metamorphic rocks, pyroxene composition as a significant rock-forming ferromagnesian silicate phase, is used to understand the processes of magma generation and crystallization conditions. Thermobarometry, which is the estimation of *P*-*T* conditions of rocks, can be used by conventional methods and pseudosection calculations. Over the past 45 year, a number of studies are focused on the *P*-*T* estimations for a single-clinopyroxene- and two-pyroxene-bearing rocks (see references therein Yavuz, 2013).

Thermobarometry estimations are not only carried on a single mineral or two mineral phases in a rock

composition, but also are obtained from the liquid-only and mineral-liquid components. Beattie (1993) presented a thermometer based on orthopyroxene-liquid equilibria using the empirical activity-composition relationships. Putirka et al. (1996) developed a series of thermobarometers for anhydrous systems including mafic igneous rocks co-existing jadeite-diopside/hedenbergite exchange equilibrium and liquid compositions based on calibrations from existing earlier data and experimentally produced new data at 8-30 kbar and 1100-1475 ^{o}C. Using new experiments, Putirka et al. (2003) proposed clinopyroxene-liquid thermobarometers for hydrous systems that consist of mafic, evolved and volatile-bearing lava compositions (up to 71.3 wt% SiO_2) based on the jadeite-diopside+hedenbergite exchange equilibria. Putirka (2008) presented two new thermometers for orthopyroxene-liquid and only- liquid components to rectify the Beattie's (1993) method in terms of over estimations for hydrous and low estimations for some anhydrous compositions. Putirka (2008) also proposed two barometers for clinopyroxene and liquid components to better describe hydrous samples using the H_2O^{liq} (wt%) composition and one barometer based on the partitioning of Al between clinopyroxene and liquid. The Jd-DiHd exchange clinopyroxene-liquid thermometers developed by Putirka et al. (1996, 2003) were subjected to global calibrations using experimental studies at P<70 kbar to reduce the temperature of uncertainties from 52-60 ^{o}C to 10-20 ^{o}C (Putirka, 2008). Masotta et al. (2013) presented new thermometer and barometer based on clinopyroxene-liquid equilibria to predict magmatic temperatures and pressures of alkaline differentiated magmas. Neave and Putirka (2017) tested the performance of commonly used clinopyroxene-liquid barometers with data from experiments on H_2O-poor tholeiites and calibrated a new barometer in the 1 atm to 20 kbar to improve the accuracy of Jd-in-clinopyroxene barometry.

Although several computer programs have been developed for pyroxene calculation and classification purposes (McHone, 1987; Gómez, 1990; Yavuz, 2001; Sturm, 2002), restricted attention was given on single-clinopyroxene and two-pyroxene thermobarometers as well as orthopyroxene-liquid and clinopyroxene-liquid thermometers and barometers. Putirka (2008) and Neave and Putirka (2017) developed Excel spreadsheets on thermobarometers for clinopyroxene-only, two-pyroxene and pyroxene-liquid analyses. Yavuz (2013) presented a Visual Basic program, called WinPyrox, for recalculation of multiple single-clinopyroxene and two-pyroxene chemical analyses, providing various single-clinopyroxene and two-pyroxene thermobarometers.

A Windows program, called WinPLtb, is developed to estimate the *P-T* conditions of pyroxene-bearing rocks based on pyroxene-liquid equilibria. Unlike the earlier WinPyrox program, the current software calculates only pyroxene-liquid thermometers and barometers using clinopyroxene and orthopyroxene analyses and liquid or whole-rock compositions equilibrated with clinopyroxene and orthopyroxene.

DESCRIPTION OF PROGRAM

Although a variety of computer programs have been published for calculation and classification of rock-forming silicate minerals in recent years (e.g. Yavuz, 1999, 2001, 2003 a,b, 2007; Yavuz et al., 2006, 2014; Locock, 2014), an increasing number of thermobarometry software based on the mineral and mineral-liquid chemistry were appeared in estimation the *P-T* conditions of igneous rocks (e.g. Soto and Soto, 1995; Yavuz, 1998; Lepage, 2003; Hora et al., 2013; Yavuz, 2013; Masotta et al., 2013; Lanari et al., 2014; Yavuz et al., 2015; Yavuz and Döner, 2017; Neave and Putirka, 2017).

WinPLtb is a compiled program developed for the Microsoft® Windows platform users. The program is intended to calculate most widely used clinopyroxene-liquid and orthopyroxene-liquid thermobarometers for pyroxene analyses associated with chemical composition of liquid or whole-rocks. Calculation of all pyroxene and liquid compositions by WinPLtb is carried out in two windows called the *Data Entry Screen* and *Calculation Screen*, respectively. A list of the calculation steps in the *Calculation Screen* of program is given in Table 1. WinPLtb presents eight binary plots for the *P-T* conditions of pyroxene-liquid equilibria. These plots are displayed by the Golden Software's Grapher program by selecting diagram types from the pull-down menu of *Graph* in the *Calculation Screen* of WinPLtb.

In pyroxene-liquid thermobarometry, calculation of pyroxene components require without normalization to total four cations. However, by selecting options from the pull-down menu of *Normalization* (Figure 1a) in the *Data Entry Screen*, the program normalizes cations on the basis of total four cations. The program separates ferric and ferrous iron contents of electron-microprobe-derived pyroxene analyses based on the Droop's (1987) method, if first option is selected from the pull-down menu of *Ferric Iron Estimation* in the *Data Entry Screen*. Similarly, by selecting second option from the pull-down menu of *Ferric Iron Estimation* (Figure 1b) in the *Data Entry Screen*, the program carries out ferric and ferrous iron separation from total FeO content based on the Papike et al.'s (1974) method. The temperature-dependent clinopyroxene-liquid barometers and pressure-dependent clinopyroxene-liquid thermometers are optionally estimated by selecting the options from pull-down menu of *Thermobarometers* (Figure 1c), provided that these input *T* (K) and *P* (kbar)

Table 1. Description of column numbers in the *Calculation Screen* window of WinPLtb program and an output Excel file.

Row	Explanations	Column Numbers
1	Major oxide clinopyroxene analyses (wt%)	1-19
2	Recalculated cations of clinopyroxene analyses *(apfu)*	20-38
3	Clinopyroxene components [from Putirka (2008)]	39-45
4	Checking for clinopyroxene composition	46
5	Blank	47
6	Major oxide orthopyroxene analyses (wt%)	48-67
7	Recalculated cations of orthopyroxene analyses *(apfu)*	68-86
8	Orthopyroxene components [from Putirka (2008)]	87-93
9	Checking for orthopyroxene composition	94
10	Blank	95
11	Major oxide (wt%) liquid (glass or whole-rock) composition equilibrated with clinopyroxene	96-110
12	Calculated liquid cation fractions equilibrated with clinopyroxene	111-123
13	Blank	124
14	Clinopyroxene-liquid barometers (kbar)	125-138
15	Clinopyroxene-liquid thermometers (^{o}C)	139-156
16	Blank	157
17	Depth (km) estimation based on clinopyroxene-liquid barometer (kbar)	158-160
18	Blank	161
19	Clinopyroxene-based hygrometer (H_2O, wt%)	162-163
20	Blank	164
21	Major oxide (wt%) liquid (glass or whole-rock) composition equilibrated with orthopyroxene	165-179
22	Calculated liquid cation fractions equilibrated with orthopyroxene	180-192
23	Blank	193
24	Orthopyroxene-liquid barometers (kbar)	194-196
25	Orthopyroxene-liquid thermometers (^{o}C)	197-199
26	Blank	200
27	Input pressure (GPa) for orthopyroxene-liquid and liquid-only thermometers	201
28	Input temperature (Kelvin) for clinopyroxene-liquid barometers	202
29	Input pressure (kbar) for clinopyroxene-liquid thermometers	203

apfu = Atoms per formula unit.

values are typed in the last two columns of the *Data Entry Screen*. By selecting the input or calculated clinopyroxene-based *P* (kbar) option from the pull-down menu of *Depth* (Figure 1d) in the *Data Entry Screen*, WinPLtb estimates depth (km) values using the density-depth models (e.g. Hill and Zucca, 1987; Mavko and Thompson, 1983 and DeBari and Greene, 2011; Prezzi et al., 2009). The program estimates clinopyroxene-based hygrometers (e.g. Armienti et al., 2013; Perinelli et al., 2016) by selecting one of option from the pull-down menu of *Hygrometers* (Figure 1e) in the *Data Entry Screen*. Calculation of pyroxene analyses are carried out on the basis of six oxygens. Selected options from the *Data Entry Screen* are displayed at the base of *Calculation Screen*.

The program comes up with a self-extracting setup file (14 Mb) by using the Inno Setup Compiler (version 5.5.9) developed by Jordan Russell (2018) (http://www.jrsoftware.org/isdl.php). WinPLtb runs as a single executable file on a computer where the Microsoft® Visual Studio (MVP) package is installed. However, with the help of necessary ".ocx" and ".dll" support files in the self-extracting setup file, the users can execute WinPLtb without requiring the MVP package. WinPLtb runs properly in a personal computer with the 32-bit operating system. An execution of program in a personal computer with the 64-bit operating system requires the registration

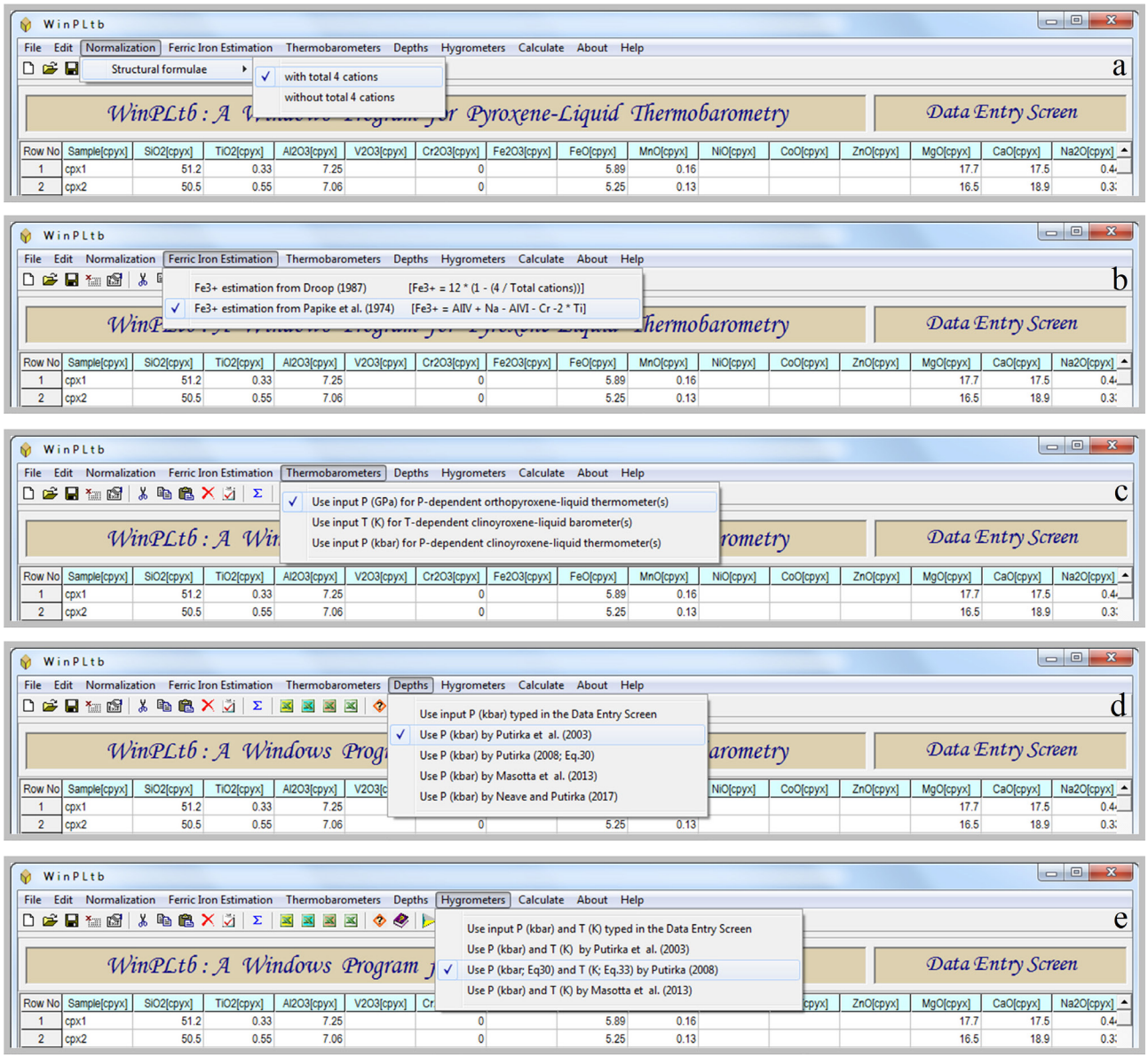

Figure 1. Screenshots of WinPLtb program showing the menu of (a) *Normalization* scheme, (b) *Ferric Iron Estimation* methods, (c) *Thermobarometers* for calculations based on the typed input *P-T* values, (d) *Depths* using the input and estimated clinopyroxene-based pressure values for depth estimations, (e) *Hygrometers* using the input and estimated clinopyroxene-liquid-based *P-T* values for water content estimations.

of MSFLEXGRD.OCX component by users just after an installation of WinPLtb (See Appendix). Following an installation of WinPLtb setup file on the computer, the start-up screen with various pull-down menus and shortcuts appears on the screen. Execution of program may also be started by clicking the WinPLtb icon from All Programs options or program icon came-up with the installation on the desktop.

Data entry of clinopyroxene, orthopyroxene and liquid compositions

The users of WinPLtb can edit pyroxene analyses obtained from wet-chemical or electron-microprobe techniques and liquid or whole-rock compositions equilibrated with pyroxene by clicking the *New* icon on the tool bar, by selecting *New File* from the pull-down menu of *File* option or pressing the Ctrl+N keys. The standard 19 and 14 variables are defined by program for calculations of pyroxene and liquid or whole-rock compositions as in

the following order in Table 2. In the *Data Entry Screen*, parameters that belong to these four groups are highlighted by the light cyan, light green, faded pink and light yellow colors (see Figure 2). Clinopyroxene, orthopyroxene and liquid compositions typed in an Excel file with the extension of ".xls" and ".xlsx" as in the order given in Table 2, can be loaded into the program's *Data Entry Screen* by clicking the *Open Excel File* option from the pull-down menu of *File*. By selecting the *Edit Excel File* option from the pull-down menu of *File*, clinopyroxene, orthopyroxene and liquid analyses can be typed in a blank Excel file (i.e. WinPLtb), stored in a different file name with the extension of ".xls" or ".xlsx", and then loaded into the program's *Data Entry Screen* by clicking the *Open Excel File* option from the pull-down menu of *File*. Additional information about data entry or similar topics can be accessed by pressing the F1 function key to display the WinPLtb.chm help file on the screen.

WORKED EXAMPLES

The following examples show how WinPLtb can be used for a variety of orthopyroxene-liquid and clinopyroxene-liquid thermobarometers in igneous rocks. Thermobarometry, hygrometry and depth estimations by program with explanations are listed in Table 3. Validity of WinPLtb outputs has been tested (see Tables 4 and 5) using data sets in Excel spreadsheets developed by authors (e.g. Masotta et al., 2013; Putirka, 2018a, b; Neave and Putirka, 2017) for their different thermobarometry models. Once the pyroxene and liquid analyses are processed by clicking the Calculate icon (i.e. ∑) in the *Data Entry Section* of the program (see Figure 2a), all estimation parameters are displayed in columns 1-199 (see Table 1) of the *Calculation Screen*. Pressing the *Ctrl+F* keys or clicking the *Open File to Calculate* option from the *Calculate* menu also executes the data processing for a selected data file with the extension of ".pyx". By clicking the *Send results to Excel file* icon in the *Calculation Screen*, all calculations can be stored in an Excel file (Output.xlsx) and then displayed by clicking the *Open and edit Excel file* icon. In an output Excel file, explanations can be displayed as comments provided that mouse cursor is on the second row of each column (see Figure 3).

Table 2. Data entry sequence of pyroxene analyses and liquid compositions in WinPLtb program.

	First Group	Second Group	Third Group	Fourth Group
Row	Clinopyroxene [i]	Orthopyroxene [j]	Liquid-clinopyroxene [k]	Liquid-orthopyroxene [l]
1	Sample[cpyx]	Sample[opyx]	Sample[lcpyx]	Sample[lopyx]
2	SiO_2[cpyx]	SiO_2[opyx]	SiO_2[lcpyx]	SiO_2[lopyx]
3	TiO_2[cpyx]	TiO_2[opyx]	TiO_2[lcpyx]	TiO_2[lopyx]
4	Al_2O_3[cpyx]	Al_2O_3[opyx]	Al_2O_3[lcpyx]	Al_2O_3[lopyx]
5	V_2O_3[cpyx]	V_2O_3[opyx]	Cr_2O_3[lcpyx]	Cr_2O_3[lopyx]
6	Cr_2O_3[cpyx]	Cr_2O_3[opyx]	$FeO_{(total)}$[lcpyx]	$FeO_{(total)}$[lopyx]
7	Fe_2O_3[cpyx]	Fe_2O_3[opyx]	MnO[lcpyx]	MnO[lopyx]
8	FeO[cpyx]	FeO[opyx]	NiO[lcpyx]	NiO[lopyx]
9	MnO[cpyx]	MnO[opyx]	MgO[lcpyx]	MgO[lopyx]
10	NiO[cpyx]	NiO[opyx]	CaO[lcpyx]	CaO[lopyx]
11	CoO[cpyx]	CoO[opyx]	Na_2O[lcpyx]	Na_2O[lopyx]
12	ZnO[cpyx]	ZnO[opyx]	K_2O[lcpyx]	K_2O[lopyx]
13	MgO[cpyx]	MgO[opyx]	P_2O_5[lcpyx]	P_2O_5[lopyx]
14	CaO[cpyx]	CaO[opyx]	H_2O[lcpyx]	H_2O[lopyx]
15	Na_2O[cpyx]	Na_2O[opyx]		
16	K_2O[cpyx]	K_2O[opyx]		
17	ZrO_2[cpyx]	ZrO_2[opyx]		
18	Sc_2O_3[cpyx]	Sc_2O_3[opyx]		
19	Li_2O[cpyx]	Li_2O[opyx]		

i [cpyx]=Sample number and content of clinopyroxene analysis; *j* [opyx]=Sample number and content of orthopyroxene analysis; *k* [lcpyx]=Sample number and content of liquid or whole-rock composition equilibrated with clinopyroxene; *l* [lopyx]=Sample number and content of liquid or whole-rock composition equilibrated with orthopyroxene.

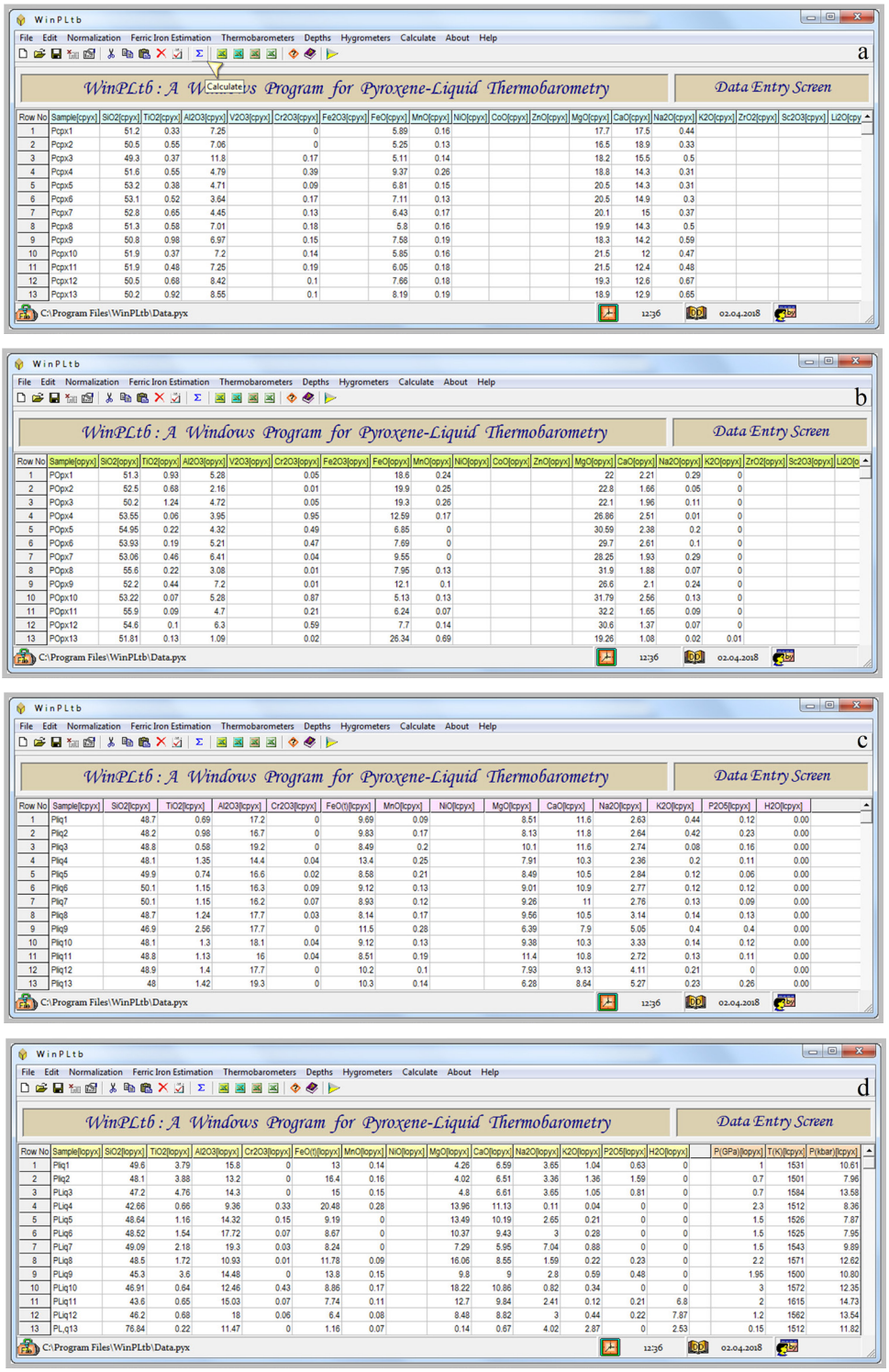

Figure 2. Screenshots of WinPLtb program showing (a) Clinopyroxene analyses with variables highlighted by light cyan color, (b) Orthopyroxene analyses with variables highlighted by light green color, (c) liquid or whole-rock compositions equilibrated with clinopyroxene with variables highlighted by faded pink color, (d) liquid or whole-rock compositions equilibrated with orthopyroxene with variables highlighted by light yellow color. Last three columns highlighted by light salmon color show the input *P-T* values typed by user to be used in estimation of the *P*-dependent orthopyroxene-liquid thermometers, as well as the *T*- and *P*-dependent clinopyroxene-liquid thermobarometers.

Table 3. Description of thermobarometry, depth and hygrometry estimations in the *Calculation Screen* window of WinPLtb program and an output Excel file.

Row	Explanations	Equation	Column	Author
1	*T*-dependent clinopyroxene-liquid barometer (*P*1, kbar) using *T*1 (K)	11	125	Putirka et al. (1996)
2	*T*-dependent clinopyroxene-liquid barometer (*P*2, kbar) using *T*1 (K)	12	126	Putirka et al. (1996)
3	*T*-dependent clinopyroxene-liquid barometer (*P*1, kbar) using *T*1 (K)	27	127	Masotta et al. (2013) after Putirka et al. (1996)
4	*T*-dependent clinopyroxene-liquid barometer (*P*2, kbar) using *T*1 (K)	28	128	Masotta et al. (2013) after Putirka et al. (1996)
5	*T*-dependent clinopyroxene-liquid barometer (*P,* kbar) using *T*1 (K) by Putirka et al. (1996)	13	129	Putirka et al. (2003)
6	*T*-dependent clinopyroxene-liquid barometer (*P*, kbar) using *T* (K) by Putirka et al. (2003)	13	130‡	Putirka et al. (2003)
7	*T*-dependent clinopyroxene-liquid barometer (*P*, kbar) using *T*1 (K) by Putirka et al. (1996)	15	131	Putirka (2008; Eq. 30)
8	*T*-dependent clinopyroxene-liquid barometer (*P*, kbar) using *T*1 (K) by Putirka et al. (1996)	16	132	Putirka (2008; Eq. 31)
9	*T*-dependent clinopyroxene-liquid barometer (*P*, kbar) using *T*1 (K) by Putirka et al. (1996)	17	133	Putirka (2008; Eq. 32b)
10	*T*-dependent clinopyroxene-liquid barometer (*P*, kbar) using *T1* (K) by Putirka et al. (1996)	18	134	Putirka (2008; Eq. 32c)
11	*T*-dependent clinopyroxene-liquid barometer (*P*, kbar) using *T*1 (K) by Putirka (2008; Eq. 32c)	29	135	Recalibration by Masotta et al. (2013)
12	Clinopyroxene-liquid barometer (*P*, kbar)	22	136	Masotta et al. (2013)
13	*T*-dependent clinopyroxene-liquid barometer (*P*, kbar) using *T* (K) by Putirka (2008; Eq. 33)	28	137	Neave and Putirka (2017)
14	*T*-dependent clinopyroxene-liquid barometer (*P*, kbar) using *T* (K) by Putirka (2008; Eq. 33)	31	138	Neave and Putirka (2017)
15	Clinopyroxene-liquid thermometer (*T*1, ºC)*	7	139	Putirka et al. (1996)
16	*P*-dependent clinopyroxene-liquid thermometer (*T*2, ºC) using *P*1 (kbar) by Putirka et al. (1996)	8	140	Putirka et al. (1996)
17	*P*-dependent clinopyroxene-liquid thermometer (*T*2, ºC) using *P* (kbar) by Putirka et al. (2003; see column number 130)	8	141‡	Putirka et al. (1996)
18	Clinopyroxene-liquid thermometer (*T*3, ºC)	9	142	Putirka et al. (1996)
19	*P*-dependent clinopyroxene-liquid thermometer (*T*4, ºC) using *P* (kbar) by Putirka et al. (2003)	10	143	Putirka et al. (1996)
20	*P*-dependent clinopyroxene-liquid saturation thermometer (ºC) using *P* (kbar) by Putirka et al. (2003; see column number 130)	Ngp	144‡	Putirka (1999)
21	Clinopyroxene-liquid thermometer (*T*1, ºC) using *T*1 (K) by Putirka et al. (1996)	23	145	Recalibration by Masotta et al. (2013)
22	*P*-dependent clinopyroxene-liquid thermometer (*T*2, ºC) using *T*2 (K) by Putirka et al. (1996) and *P*2 (kbar) by Masotta et al. (2013)	24	146	Recalibration by Masotta et al. (2013)
23	Clinopyroxene-liquid thermometer (*T*3, ºC) using *T*3 (K) by Putirka et al. (1996)	25	147	Recalibration by Masotta et al. (2013)
24	*P*-dependent clinopyroxene-liquid thermometer (*T*4, ºC) using *T*4 (K) by Putirka et al. (1996) and *P*2 (kbar) by Masotta et al. (2013)	26	148	Recalibration by Masotta et al. (2013)

Table 3. ... Continued

Row	Explanations	Equation	Column	Author
25	*P*-dependent clinopyroxene-liquid thermometer (*T*, °C) using *P* (kbar) by Putirka et al. (2003)	14	149	Putirka et al. (2003)
26	*P*-dependent clinopyroxene-liquid thermometer (*T*, °C) using *P* (kbar) by Putirka et al. (2003)	19	150	Putirka (2008; Eq. 33)
27	*P*-dependent clinopyroxene-liquid thermometer (*T*, °C) using *P*1 (kbar) by Putirka et al. (1996)	19	151ǂ	Putirka (2008; Eq. 33)
28	*P*-dependent clinopyroxene-liquid thermometer (*T*, °C) using *P* (kbar) by Neave and Putirka (2017)	19	152	Putirka (2008; Eq. 33)
29	*P*-dependent clinopyroxene-liquid thermometer (*T*, °C) using *P*2 (kbar) by Masotta et al. (2013)	30	153	Recalibration by Masotta et al. (2013)
30	*P*-dependent clinopyroxene-liquid thermometer (*T*, °C) using *P* (kbar) by Putirka et al. (2003)	20	154	Putirka (2008; Eq. 34)
31	*P*-dependent clinopyroxene-liquid thermometer (*T*, °C) using *P*1 (kbar) by Putirka et al. (1996)	20	155ǂ	Putirka (2008; Eq. 34)
32	Clinopyroxene-liquid thermometer (*T*,°C)	21	156	Masotta et al. (2013)
33	Depth (km) estimation based on the clinopyroxene-liquid barometer (*P*, kbar) using the density model	32	158	Hill and Zucca (1987)
34	Depth (km) estimation based on the clinopyroxene-liquid barometer (*P*, kbar) using the density-depth models	33	159	Mavko and Thompson (1983) and DeBari and Greene (2011)
35	Depth (km) estimation based on the clinopyroxene-liquid barometer (*P*, kbar) using the density-depth model	34	160	Prezzi et al. (2009)
36	Clinopyroxene-based hygrometer (H_2O, wt%)	35	162	Armienti et al. (2013)
37	Clinopyroxene-based hygrometer (H_2O, wt%)	36	163	Perinelli et al. (2016)
38	*T*-dependent orthopyroxene-liquid barometer (*P*, kbar)	4	194	Putirka (2008; Eq. 29a)
39	*T*-dependent orthopyroxene-liquid barometer (*P*, kbar)	5	195	Putirka (2008; Eq. 29b)
40	*T*-dependent orthopyroxene-liquid barometer (*P*, kbar)	6	196	Putirka (2008; Eq. 29c)
41	*P*-dependent orthopyroxene-liquid thermometer (*T*, °C) using input orthopyroxene-liquid *P* (Gpa)	1	197	Beattie (1993)
42	*P*-dependent orthopyroxene-liquid thermometer (*T*1, °C) using input orthopyroxene-liquid *P* (Gpa)	2	198	Putirka (2008; Eq. 28a)
43	*P*-dependent liquid thermometer (*T*2, °C) using input orthopyroxene-liquid *P* (Gpa)	3	199	Putirka (2008; Eq. 28b)
44	Input pressure (*P*, GPa) for *P*-dependent orthopyroxene-liquid thermometers	-	201	-
45	Input temperature (*T*, K) for *T*-dependent clinopyroxene-liquid barometers	-	202	-
46	Input pressure (*P*, kbar) for *P*-dependent clinopyroxene-liquid thermometers	-	203	-

Notes: Explanations in this table can be displayed in program's Excel file (i.e. Output.xlsx) as comments, if mouse cursor is on the second row of each column; (*) = Temperature values in the *Calculation Screen* of program and output Excel file were converted from kelvin (K) to celsius (°C); (ǂ) = *P-T* values in these columns were calculated based on an iterative approach; Ngp = Not given in paper.

Table 4. Orthopyroxene-liquid thermobarometer estimations by WinPLtb program.

Row	Orthopyroxene compositions	Popx1	Popx2	Popx3	Popx4	Popx5	Popx6	Popx7	Popx8	Popx9	Popx10	Popx11	Popx12	Popx13
1	SiO_2	51.30	52.50	50.20	53.55	54.95	53.93	53.06	55.60	52.20	53.22	55.90	54.60	51.81
2	TiO_2	0.93	0.68	1.24	0.06	0.22	0.19	0.46	0.22	0.44	0.07	0.09	0.10	0.13
3	Al_2O_3	5.28	2.16	4.72	3.95	4.32	5.21	6.41	3.08	7.20	5.28	4.70	6.30	1.09
4	Cr_2O_3	0.05	0.01	0.05	0.95	0.49	0.47	0.04	0.01	0.01	0.87	0.21	0.59	0.02
5	FeO_{Total}	18.60	19.90	19.30	12.59	6.85	7.69	9.55	7.95	12.10	5.13	6.24	7.70	26.34
6	MnO	0.24	0.25	0.26	0.17	0.00	0.00	0.00	0.13	0.10	0.13	0.07	0.14	0.69
7	MgO	22.00	22.80	22.10	26.86	30.59	29.70	28.25	31.90	26.60	31.79	32.20	30.60	19.26
8	CaO	2.21	1.66	1.96	2.51	2.38	2.61	1.93	1.88	2.10	2.56	1.65	1.37	1.08
9	Na_2O	0.29	0.05	0.11	0.01	0.20	0.10	0.29	0.07	0.24	0.13	0.09	0.07	0.02
10	Total (wt%)	100.90	100.01	99.94	100.65	100.00	99.90	99.99	100.84	100.99	99.18	101.15	101.47	100.45
	Cations on the basis of 6 oxygens													
11	Si	1.870	1.938	1.857	1.904	1.911	1.887	1.866	1.924	1.841	1.861	1.910	1.873	1.964
12	Ti	0.026	0.019	0.035	0.002	0.006	0.005	0.012	0.006	0.012	0.002	0.002	0.003	0.004
13	Al	0.227	0.094	0.206	0.166	0.177	0.215	0.266	0.126	0.299	0.218	0.189	0.255	0.049
14	Cr	0.001	0.000	0.001	0.027	0.013	0.013	0.001	0.000	0.000	0.024	0.006	0.016	0.001
15	Fe^{3+}	0.002	0.000	0.026	0.000	0.000	0.000	0.000	0.029	0.018	0.061	0.000	0.000	0.026
16	Fe^{2+}	0.565	0.614	0.571	0.374	0.199	0.225	0.281	0.201	0.339	0.089	0.178	0.221	0.809
17	Mn	0.007	0.008	0.008	0.005	0.000	0.000	0.000	0.004	0.003	0.004	0.002	0.004	0.022
18	Mg	1.196	1.255	1.219	1.424	1.586	1.549	1.481	1.646	1.398	1.657	1.640	1.565	1.088
19	Ca	0.086	0.066	0.078	0.096	0.089	0.098	0.073	0.070	0.079	0.096	0.060	0.050	0.044
20	Na	0.020	0.004	0.008	0.001	0.013	0.007	0.020	0.005	0.016	0.009	0.006	0.005	0.001
21	Total (*apfu*)	4.001	3.998	4.009	3.998	3.995	3.998	3.999	4.010	4.006	4.021	3.994	3.991	4.009
	Orthopyroxene components													
22	$NaAlSi_2O_6$	0.020	0.004	0.008	0.001	0.013	0.007	0.020	0.005	0.016	0.009	0.006	0.005	0.001
23	$FmTiAlSiO_6$	0.026	0.019	0.035	0.002	0.006	0.005	0.012	0.006	0.012	0.002	0.002	0.003	0.004
24	$CrAl_2SiO_6$	0.001	0.000	0.001	0.027	0.013	0.013	0.001	0.000	0.000	0.024	0.006	0.016	0.001
25	$FmAl_2SiO_6$	0.075	0.028	0.054	0.043	0.061	0.082	0.110	0.045	0.123	0.046	0.087	0.107	0.011
26	$CaFmSi_2O_6$	0.086	0.066	0.078	0.096	0.089	0.098	0.073	0.070	0.079	0.096	0.060	0.050	0.044
27	$Fm_2Si_2O_6$	0.792	0.882	0.829	0.832	0.815	0.795	0.783	0.880	0.772	0.834	0.835	0.815	0.944
28	Total	1.000	0.999	1.004	0.999	0.997	0.999	0.999	1.005	1.003	1.010	0.997	0.996	1.004
	Liquid compositions													
29	SiO_2	49.60	48.10	47.20	42.66	48.64	48.52	49.09	48.50	45.30	46.91	43.60	46.20	76.84
30	TiO_2	3.79	3.88	4.76	0.66	1.16	1.54	2.18	1.72	3.60	0.64	0.65	0.68	0.22
31	Al_2O_3	15.80	13.20	14.30	9.36	14.32	17.72	19.30	10.93	14.48	12.46	15.03	18.00	11.47
32	Cr_2O_3	0.00	0.00	0.00	0.33	0.15	0.07	0.03	0.01	0.00	0.43	0.07	0.06	0.00
33	FeO_{Total}	13.00	16.40	15.00	20.48	9.19	8.67	8.24	11.78	13.80	8.86	7.74	6.40	1.16
34	MnO	0.14	0.16	0.15	0.28	0.00	0.00	0.00	0.09	0.15	0.17	0.11	0.08	0.07
35	MgO	4.26	4.02	4.80	13.96	13.49	10.37	7.29	16.06	9.80	18.22	12.70	8.48	0.14
36	CaO	6.59	6.51	6.61	11.13	10.19	9.43	5.95	8.55	9.00	10.86	9.84	8.82	0.67
37	Na_2O	3.65	3.36	3.65	0.11	2.65	3.00	7.04	1.59	2.80	0.82	2.41	3.00	4.02
38	K_2O	1.04	1.36	1.05	0.04	0.21	0.28	0.88	0.22	0.59	0.34	0.12	0.44	2.87
39	P_2O_5	0.63	1.59	0.81	0.00	0.00	0.00	0.00	0.23	0.48	0.00	0.21	0.22	0.00
40	H_2O	0.00	0.00	0.00	0.00	0.00	0.00	0.00	0.00	0.00	0.00	6.80	7.87	2.53
41	Total (wt%)	98.50	98.58	98.33	99.01	100.00	99.60	100.00	99.68	100.00	99.71	99.28	100.25	99.99

Table 4. ... Continued

Row	Orthopyroxene compositions	Popx1	Popx2	Popx3	Popx4	Popx5	Popx6	Popx7	Popx8	Popx9	Popx10	Popx11	Popx12	Popx13
	Cation fractions of liquid compositions													
42	X_{SiO2}	0.4760	0.4700	0.4570	0.4070	0.4400	0.4430	0.4370	0.4440	0.4220	0.4230	0.4240	0.4530	0.7390
43	X_{TiO2}	0.0270	0.0290	0.0350	0.0050	0.0080	0.0110	0.0150	0.0120	0.0250	0.0040	0.0050	0.0050	0.0020
44	$X_{AlO1.5}$	0.1790	0.1520	0.1630	0.1050	0.1530	0.1910	0.2020	0.1180	0.1590	0.1330	0.1720	0.2080	0.1300
45	$X_{CrO1.5}$	0.0000	0.0000	0.0000	0.0020	0.0010	0.0010	0.0000	0.0000	0.0000	0.0030	0.0010	0.0000	0.0000
46	X_{FeO}	0.1040	0.1340	0.1210	0.1630	0.0690	0.0660	0.0610	0.0900	0.1070	0.0670	0.0630	0.0520	0.0090
47	X_{MnO}	0.0010	0.0010	0.0010	0.0020	0.0000	0.0000	0.0000	0.0010	0.0010	0.0010	0.0010	0.0010	0.0010
48	X_{MgO}	0.0610	0.0590	0.0690	0.1990	0.1820	0.1410	0.0970	0.2190	0.1360	0.2450	0.1840	0.1240	0.0020
49	X_{CaO}	0.0680	0.0680	0.0690	0.1140	0.0990	0.0920	0.0570	0.0840	0.0900	0.1050	0.1030	0.0930	0.0070
50	$X_{NaO0.5}$	0.0680	0.0640	0.0690	0.0020	0.0460	0.0530	0.1210	0.0280	0.0510	0.0140	0.0450	0.0570	0.0750
51	$X_{KO0.5}$	0.0130	0.0170	0.0130	0.0000	0.0020	0.0030	0.0100	0.0030	0.0070	0.0040	0.0010	0.0060	0.0350
53	$X_{PO2.5}$	0.0030	0.0070	0.0030	0.0000	0.0000	0.0000	0.0000	0.0010	0.0020	0.0000	0.0010	0.0010	0.0000
54	Total	1.000	1.001	1.000	0.999	1.000	1.001	1.000	1.000	1.000	0.999	1.000	1.000	1.000
	Orthopyroxene- liquid barometers (kbar)													
55	$P1_{P08\_Eq29a\_T1P08\_Eq28a}$	1.16	0.77	1.03	1.72	1.58	1.25	1.73	1.67	1.81	2.13	1.85	1.51	n.d.
56	$P2_{P08\_Eq29b\_T1P08\_Eq28a}$	1.14	0.95	1.20	2.08	1.56	1.29	1.37	2.05	1.86	2.48	1.53	1.16	0.15
57	$P3_{P08\_Eq29c\_T1P08\_Eq28a}$	0.91	0.26	0.91	2.30	1.79	1.47	1.17	2.36	1.58	3.74	1.23	0.85	0.64
	Orthopyroxene-liquid thermometers (°C)													
58	T_{B93_PInput}	1194	1174	1181	1449	1383	1331	1316	1485	1350	1554	1413	1292	1083
59	$T1_{P08\_Eq28a\_PInput}$	1195	1197	1197	1479	1376	1321	1251	1495	1365	1611	1254	1130	844
60	$T2_{P08\_Eq28b\_PInput}$	1169	1147	1172	1489	1388	1330	1259	1480	1353	1508	1257	1139	868

Notes: Orthopyroxene (rows 1 to 9) and liquid (rows 29 to 40) compositions are taken from Excel sheets of Putirka (2016). *apfu*=atomic per formula unit; Ferric iron (Fe^{3+}, see row 15) calculation is from Droop (1987) by clicking the *Ferric iron estimation* option in the *Data Entry Screen*; Orthopyroxene component ($NaAlSi_2O_6$ to $Fm_2Si_2O_6$ in rows between 22 and 27) estimation method is taken from Putirka (2008); X_{SiO_2} to $X_{PO2.5}$=Cation fractions of liquid (glass or whole-rock, etc.) compositions (see rows 42 to 53); $P1_{P08\_Eq29a\_T1P08}$ (row 55) from Putirka (2008) using $T1$ (°C; Eq.28a) by Putirka (2008), $P2_{P08\_Eq29b\_T1P08\_Eq28a}$ (row 56) from Putirka (2008) using $T1$ (°C; Eq.28a) by Putirka (2008), $P3_{P08\_Eq29c\_T1P08\_Eq28a}$ (row 57) from Putirka (2008) using $T1$ (°C; Eq.28a) by Putirka (2008); T_{B93_PInput} (row 58) from Beattie (1993) using input P (GPa), $T1_{P08\_Eq28a\_PInput}$ (row 59) from Putirka (2008) using input P (GPa), $T2_{P08\_Eq28b\_PInput}$ (row 60) from Putirka (2008) using input P (GPa); n.d.=not determined.

Thermobarometry

Thermobarometer is the estimation procedure of temperature (°C) and pressure (kbar) conditions of metamorphic and igneous rocks based on the mineral and liquid components or phases. An application of many experimentally calibrated thermodynamic models for estimating the equilibration temperatures and pressures of natural samples may not be successful if the textural evidence for equilibrium between the phases of interest is ignored (Blundy and Cashman, 2008). In general, a practical good thermometer uses reactions with large enthalpy changes (ΔH_r), while a barometer requires a reaction with large-volume changes (ΔV_r). These reactions are temperature-dependent, and show often steep slopes in the *P-T* diagrams. In thermobarometric studies, thermodynamic data used to estimate the equilibrium constant (K_{eq}) may be obtained by calorimetric studies or using empirical equations. In both cases, the relationship between activity and composition *(a-X)* is essential to define the equilibrium constant from natural mineral or melt compositions (Blundy and Cashman, 2008). Clinopyroxenes are widespread in igneous rocks and their crystal-chemical compositions play an important role in estimating the *P-T* conditions. Consequently, a great number of thermometers and barometers that use single-clinopyroxene and two-pyroxene compositions (see references therein Yavuz, 2013) have been developed and used by earth scientists in understanding the thermobarometric structure and history of the Earth's crust and upper mantle.

Table 5. Clinopyroxene-liquid thermobarometers, clinopyroxene-based hygrometers and depth estimations by WinPLtb program.

Row	Clinopyroxene compositions	Pcpx1	Pcpx2	Pcpx3	Pcpx4	Pcpx5	Pcpx6	Pcpx7	Pcpx8	Pcpx9	Pcpx10	Pcpx11	Pcpx12	Pcpx3
1	SiO_2	51.20	50.50	49.30	51.60	53.20	53.10	52.80	51.30	50.80	51.90	51.90	50.50	50.20
2	TiO_2	0.33	0.55	0.37	0.55	0.38	0.52	0.65	0.58	0.98	0.37	0.48	0.68	0.92
3	Al_2O_3	7.25	7.06	11.80	4.79	4.71	3.64	4.45	7.01	6.97	7.20	7.25	8.42	8.55
4	Cr_2O_3	0.00	0.00	0.17	0.39	0.09	0.17	0.13	0.18	0.15	0.14	0.19	0.10	0.10
5	FeO_{Total}	5.89	5.25	5.11	9.37	6.81	7.11	6.43	5.80	7.58	5.85	6.05	7.66	8.19
6	MnO	0.16	0.13	0.14	0.26	0.15	0.13	0.17	0.16	0.19	0.16	0.18	0.18	0.19
7	MgO	17.70	16.50	18.20	18.80	20.50	20.50	20.10	19.90	18.30	21.50	21.50	19.30	18.90
8	CaO	17.50	18.90	15.50	14.30	14.30	14.90	15.00	14.30	14.20	12.00	12.40	12.60	12.90
9	Na_2O	0.44	0.33	0.50	0.31	0.31	0.30	0.37	0.50	0.59	0.47	0.48	0.67	0.65
10	Total (wt%)	100.47	99.22	101.09	100.37	100.45	100.37	100.10	99.73	99.76	99.59	100.43	100.11	100.60
	Cations on the basis of 6 oxygens													
11	Si	1.847	1.848	1.752	1.880	1.907	1.914	1.903	1.848	1.846	1.858	1.847	1.820	1.807
12	Ti	0.009	0.015	0.010	0.015	0.010	0.014	0.018	0.016	0.027	0.010	0.013	0.018	0.025
13	Al	0.308	0.304	0.494	0.206	0.199	0.155	0.189	0.298	0.298	0.304	0.304	0.358	0.363
14	Cr	0.000	0.000	0.005	0.011	0.003	0.005	0.004	0.005	0.004	0.004	0.005	0.003	0.003
15	Fe^{3+}	0.016	0.000	0.017	0.022	0.000	0.009	0.000	0.006	0.000	0.000	0.005	0.015	0.023
16	Fe^{2+}	0.161	0.171	0.134	0.264	0.225	0.205	0.204	0.168	0.240	0.190	0.175	0.216	0.224
17	Mn	0.005	0.004	0.004	0.008	0.005	0.004	0.005	0.005	0.006	0.005	0.005	0.005	0.006
18	Mg	0.952	0.900	0.964	1.021	1.095	1.101	1.080	1.069	0.991	1.147	1.141	1.037	1.014
19	Ca	0.676	0.741	0.590	0.558	0.549	0.575	0.579	0.552	0.553	0.460	0.473	0.486	0.498
20	Na	0.031	0.023	0.034	0.022	0.022	0.021	0.026	0.035	0.042	0.033	0.033	0.047	0.045
21	Total *(apfu)*	4.005	4.007	4.006	4.007	4.014	4.003	4.007	4.002	4.006	4.010	4.002	4.005	4.008
	Clinopyroxene components													
22	Jd	0.031	0.023	0.034	0.022	0.022	0.021	0.026	0.035	0.042	0.033	0.033	0.047	0.045
23	CaTs	0.124	0.129	0.212	0.064	0.084	0.047	0.066	0.111	0.103	0.129	0.118	0.131	0.125
24	CaTi	0.014	0.012	0.018	0.028	0.005	0.020	0.016	0.020	0.026	0.007	0.017	0.025	0.034
25	CrCaTs	0.000	0.000	0.002	0.006	0.001	0.002	0.002	0.003	0.002	0.002	0.003	0.001	0.001
26	DiHd	0.538	0.600	0.358	0.461	0.459	0.506	0.496	0.418	0.422	0.323	0.335	0.330	0.337
27	EnFs	0.296	0.230	0.379	0.423	0.420	0.405	0.389	0.413	0.400	0.500	0.493	0.469	0.462
28	Total	1.003	0.995	1.004	1.003	0.991	1.001	0.994	1.000	0.994	0.993	0.999	1.002	1.005
	Liquid compositions													
29	SiO_2	48.70	48.20	48.80	48.10	49.90	50.10	50.10	48.70	46.90	48.10	48.80	48.90	48.00
30	TiO_2	0.69	0.98	0.58	1.35	0.74	1.15	1.15	1.24	2.56	1.30	1.13	1.40	1.42
31	Al_2O_3	17.20	16.70	19.20	14.40	16.60	16.30	16.20	17.70	17.70	18.10	16.00	17.70	19.30
32	Cr_2O_3	0.00	0.00	0.00	0.04	0.02	0.09	0.07	0.03	0.00	0.04	0.04	0.00	0.00
33	FeO_{Total}	9.69	9.83	8.49	13.40	8.58	9.12	8.93	8.14	11.50	9.12	8.51	10.20	10.30
34	MnO	0.09	0.17	0.20	0.25	0.21	0.13	0.12	0.17	0.28	0.13	0.19	0.10	0.14
35	MgO	8.51	8.13	10.10	7.91	8.49	9.01	9.26	9.56	6.39	9.38	11.40	7.93	6.28
36	CaO	11.60	11.80	11.60	10.30	10.50	10.90	11.00	10.50	7.90	10.30	10.80	9.13	8.64
37	Na_2O	2.63	2.64	2.74	2.36	2.84	2.77	2.76	3.14	5.05	3.33	2.72	4.11	5.27
38	K_2O	0.44	0.42	0.08	0.20	0.12	0.12	0.13	0.14	0.40	0.14	0.13	0.21	0.23
39	P_2O_5	0.12	0.23	0.16	0.11	0.06	0.12	0.09	0.13	0.40	0.12	0.11	0.00	0.26
40	Total (wt%)	99.67	99.10	101.95	98.42	98.06	99.81	99.81	99.45	99.08	100.06	99.83	99.68	99.84

Table 5. ... Continued

Row	Clinopyroxene compositions	Pcpx1	Pcpx2	Pcpx3	Pcpx4	Pcpx5	Pcpx6	Pcpx7	Pcpx8	Pcpx9	Pcpx10	Pcpx11	Pcpx12	Pcpx3
	Cation fractions of liquid compositions													
41	X_{SiO_2}	0.449	0.448	0.435	0.457	0.466	0.461	0.460	0.445	0.434	0.438	0.444	0.448	0.437
42	X_{TiO_2}	0.005	0.007	0.004	0.010	0.005	0.008	0.008	0.009	0.018	0.009	0.008	0.010	0.010
43	$X_{AlO_{1.5}}$	0.187	0.183	0.202	0.161	0.183	0.177	0.175	0.191	0.193	0.194	0.172	0.191	0.207
44	$X_{CrO_{1.5}}$	0.000	0.000	0.000	0.000	0.000	0.001	0.001	0.000	0.000	0.000	0.000	0.000	0.000
45	X_{FeO}	0.075	0.076	0.063	0.106	0.067	0.070	0.069	0.062	0.089	0.069	0.065	0.078	0.078
46	X_{MnO}	0.001	0.001	0.002	0.002	0.002	0.001	0.001	0.001	0.002	0.001	0.001	0.001	0.001
47	X_{MgO}	0.117	0.113	0.134	0.112	0.118	0.124	0.127	0.130	0.088	0.127	0.155	0.108	0.085
48	X_{CaO}	0.115	0.118	0.111	0.105	0.105	0.107	0.108	0.103	0.078	0.100	0.105	0.090	0.084
49	$X_{NaO_{0.5}}$	0.047	0.048	0.047	0.043	0.051	0.049	0.049	0.056	0.091	0.059	0.048	0.073	0.093
50	$X_{KO_{0.5}}$	0.005	0.005	0.001	0.002	0.001	0.001	0.002	0.002	0.005	0.002	0.002	0.002	0.003
51	$X_{PO_{2.5}}$	0.001	0.002	0.001	0.001	0.000	0.001	0.001	0.001	0.003	0.001	0.001	0.000	0.002
52	Total	1.002	1.001	1.000	0.999	0.998	1.000	1.001	1.000	1.001	1.000	1.001	1.001	1.000
	Clinopyroxene-liquid barometers (kbar)													
53	$P1_{P96\_T1P96}$	10.61	7.96	13.58	8.36	7.87	7.95	9.89	12.62	10.80	12.35	14.73	13.54	11.82
54	$P2_{P96\_T1P96}$	11.03	8.38	13.99	8.75	8.28	8.38	10.31	12.96	10.10	12.64	15.14	13.52	10.77
55	$P1_{M13\_T1M13\_P96}$	6.30	5.85	6.61	5.79	5.53	5.65	6.03	6.35	5.47	6.13	6.75	6.15	5.54
56	$P2_{M13\_T1M13\_P96}$	6.35	5.99	6.53	6.13	5.67	5.83	6.16	6.23	5.06	5.98	6.78	5.82	5.02
57	P_{P03_T1P96}	9.49	7.10	13.18	8.25	7.50	7.78	9.30	12.48	12.11	12.60	14.72	13.24	11.41
58	$P_{P03\_TP03\_Iteratively}$	9.35	7.57	13.24	9.31	8.04	8.25	9.70	12.43	11.44	12.91	15.39	13.36	11.14
59	$P_{P08\_Eq30\_T1P96}$	8.64	6.22	13.23	7.85	7.73	7.54	9.21	11.72	9.79	11.91	14.10	12.87	11.33
60	$P_{P08\_Eq31\_TT1P96}$	10.31	8.14	14.50	8.80	8.78	8.15	9.86	13.01	11.30	13.32	15.22	14.46	11.93
61	$P_{P08\_Eq32b\_T1P96}$	10.15	8.17	11.35	7.74	9.05	7.67	9.41	11.73	9.57	12.20	13.65	12.27	9.77
62	$P_{P08\_Eq32c\_T1P96}$	9.36	7.57	14.19	7.99	7.87	7.88	9.28	12.63	10.30	11.87	15.59	13.67	11.24
63	$P_{M13\_Eq32c\_T1P96}$	7.86	7.45	9.11	7.02	7.28	7.23	7.67	8.34	6.60	8.04	9.24	8.12	7.14
64	P_{M13}	7.33	6.05	8.45	6.90	6.01	6.31	7.02	7.77	5.86	6.93	9.05	7.59	6.10
65	$P_{NP17\_TP08\_Eq33}$	9.11	6.50	12.94	6.41	6.41	5.93	7.46	10.95	11.01	11.83	11.88	12.83	13.08
66	$P_{NP17\_TP08\_Eq33\_Iteratively}$	8.47	6.62	12.44	6.71	6.34	5.85	7.24	10.59	10.94	11.72	11.65	12.73	13.17
	Clinopyroxene-liquid thermometers (°C)*													
67	$T1_{P96}$	1257	1228	1311	1238	1253	1252	1270	1298	1226	1299	1341	1289	1239
68	$T2_{P96\_P1P96}$	1263	1232	1313	1234	1247	1246	1267	1298	1231	1295	1337	1289	1246
69	$T2_{P96\_PP03\_Iteratively}$	1257	1230	1311	1238	1248	1248	1267	1297	1234	1298	1341	1288	1243
70	$T3_{P96}$	1274	1270	1320	1257	1278	1258	1279	1296	1225	1301	1349	1281	1233
71	$T4_{P96\_PP03}$	1236	1218	1278	1216	1229	1228	1245	1270	1223	1267	1308	1258	1221
72	$T_{P99\_PP03\_Iteratively}$	1267	1247	1317	1269	1263	1267	1278	1303	1251	1307	1342	1292	1244
73	$T1_{M13\_T1P96}$	1067	1064	1082	1044	1069	1070	1073	1078	1030	1072	1086	1055	1038
74	$T2_{M13\_P2M13}$	1016	1017	1028	998	1026	1024	1024	1028	997	1026	1029	1013	1006
75	$T3_{M13\_T3P96}$	1015	1006	1055	960	1014	1001	1005	1035	994	1036	1022	1017	1017
76	$T4_{M13\_P2M13}$	898	898	933	848	914	896	891	920	913	928	889	915	940
77	T_{P03_PP03}	1267	1241	1322	1267	1269	1267	1285	1300	1203	1311	1366	1289	1227
78	$T_{P08\_Eq33\_PP03}$	1250	1221	1298	1231	1240	1249	1269	1299	1231	1301	1346	1285	1244
79	$T_{P08\_Eq33\_P1P96\_Iteratively}$	1192	1226	1264	1251	1249	1248	1260	1280	1229	1290	1327	1290	1258
80	$T_{P08\_Eq33\_PNP17}$	1192	1233	1255	1260	1234	1240	1248	1267	1224	1291	1325	1276	1253
81	$T_{P2M13\_Eq33\_PP08}$	1264	1295	1262	1258	1280	1313	1315	1304	1204	1285	1313	1232	1190
82	$T_{P08\_Eq34\_PP03}$	1261	1236	1307	1241	1240	1247	1265	1294	1239	1290	1334	1276	1233
83	$T_{P08\_Eq34\_P1P96\_Iteratively}$	1169	1236	1258	1272	1261	1251	1251	1261	1230	1273	1300	1274	1247
84	T_{M13}	1174	1140	1498	1229	1273	1231	1252	1406	1343	1698	1680	1555	1460

Table 5. ... Continued

Row	Clinopyroxene compositions	Pcpx1	Pcpx2	Pcpx3	Pcpx4	Pcpx5	Pcpx6	Pcpx7	Pcpx8	Pcpx9	Pcpx10	Pcpx11	Pcpx12	Pcpx3
	Clinopyroxene-based hygrometers (H_2O, wt%)													
85	Input *P* (kbar)	10.61	7.96	13.58	8.36	7.87	7.95	9.89	12.62	10.80	12.35	14.73	13.54	11.82
86	Input *T* (K)	1531	1501	1585	1512	1527	1525	1543	1571	1500	1572	1615	1562	1512
87	H_{A13}	2.86	3.18	2.08	1.94	2.49	2.31	2.42	2.12	2.10	1.94	1.73	1.76	1.58
88	H_{P16}	0.94	1.49	0.26	1.00	0.77	0.72	0.75	0.95	0.63	1.71	2.02	1.35	1.06
	Depth (km) estimations based on clinopyroxene-liquid barometer[ǂ]													
89	D_{HZ87}	22.84	19.45	25.53	21.72	19.34	20.17	22.05	23.92	18.92	21.80	26.84	23.49	19.59
90	D_{MT83_DBG11}	26.25	21.89	30.03	24.78	21.75	22.78	25.20	27.73	21.23	24.88	32.02	27.13	22.06
91	D_{P09}	27.51	22.89	31.52	25.95	22.74	23.84	26.40	29.08	22.20	26.05	33.63	28.45	23.07

Notes: (*)=Clinopyroxene-liquid thermometers were converted from Kelvin (K) to santigrade (°C); (ǂ)=Clinopyroxene-liquid baramometer developed by Masotta et al. (2013) was used in depth estimations; Clinopyroxene (rows 1 to 9) and liquid (rows 29 to 39) compositions are taken from Excel sheets of Putirka (2016). *apfu*=atomic per formula unit; Ferric iron (Fe^{3+}, see row 15) calculation is from Droop (1987) by clicking the *Ferric iron estimation* option in the *Data Entry Screen*; Clinopyroxene component (Jd to EnFs in rows between 22 and 27) estimation method is taken from Putirka (2008); X_{SiO_2} to $X_{PO2.5}$=Cation fractions of liquid (glass or whole-rock, etc.) compositions (see rows 41 to 51); $P1_{P96\_T1P96}$ (row 53) from Putirka et al. (1996) using *T*1 (°C) by Putirka et al. (1996), $P2_{P96\_T1P96}$ (row 54) from Putirka et al. (1996) using *T*1 (°C) by Putirka et al. (1996), $P1_{M13\_T1M13\_P96}$ (row 55) from Masotta et al. (2013) using recalibrated *T*1 (°C) by Masotta et al. (2013) after Putirka et al. (1996), $P2_{M13\_T1M13\_P96}$ (row 56) from Masotta et al. (2013) using recalibrated *T*1 (°C) by Masotta et al. (2013) after Putirka et al. (1996), P_{P03_T1P96} (row 57) from Putirka et al. (2003) using *T*1 (°C) by Putirka et al. (1996), $P_{P03\_TP03\_Iteratively}$ (row 58) from Putirka et al. (2003) using *T* (°C) by Putirka et al. (2003), $P_{P08\_Eq30\_T1P96}$ (row 59) from Putirka (2008; Equation 30) using *T*1 (°C) by Putirka et al. (1996), $P_{P08\_Eq31\_T1P96}$ (row 60) from Putirka (2008; Equation 31) using *T*1 (°C) by Putirka et al. (1996), $P_{P08\_Eq32b\_T1P96}$ (row 61) from Putirka (2008; Equation 32b) using *T*1 (°C) by Putirka et al. (1996), $P_{P08\_Eq32c\_T1P96}$ (row 62) from Putirka (2008; Equation 32c) using *T*1 (°C) by Putirka et al. (1996), $P_{M13\_Eq32c\_T1P96}$ (row 63) from Masotta et al. (2013) using recalibrated *T* (°C; Equation 32c) by Masotta et al. (2013) after Putirka et al. (1996), P_{M13} (row 64) from Masotta et al. (2013), $P_{NP17\_TP08\_Eq33}$ (row 65) from Neave and Putirka (2017) using *T* (°C; Equation 33) by Putirka (2008), $P_{NP17\_TP08\_Eq33\_Iteratively}$ (row 66) from Neave and Putirka (2017) using *T* (°C; Equation 33) by Putirka (2008); $T1_{P96}$ (row 67) from Putirka et al. (1996), $T2_{P96\_P1P96}$ (row 68) from Putirka et al. (1996) using *P*1 (kbar) by Putirka et al. (1996), $T2_{P96\_PP03\_Iteratively}$ (row 69) from Putirka et al. (1996) using *P* (kbar) by Putirka et al. (2003), $T3_{P96}$ (row 70) from Putirka et al. (1996), $T4_{P96\_PP03}$ (row 71) from Putirka et al. (1996) using *P* (kbar) by Putirka et al. (2003), $T_{P99\_PP03\_Iteratively}$ (row 72; clinopyroxene-liquid saturation temperature) from Putirka (1999) using *P* (kbar) by Putirka et al. (2003), $T1_{M13\_T1P96}$ (row 73; recalibrated temperature after Putirka et al., 1996) from Masotta et al. (2013), $T2_{M13\_P2M13}$ (row 74) from Masotta et al. (2013) using *P*2 (kbar) by Masotta et al. (2013) after Putirka et al. (1996; i.e. *T*2), $T3_{M13\_T3P96}$ (row 75; recalibrated temperature after Putirka et al., 1996) from Masotta et al. (2013), $T4_{M13\_P2M13}$ (row 76) from Masotta et al. (2013) using *P*2 (kbar) by Masotta et al. (2013) after Putirka et al. (1996; i.e. *T*4), T_{P03_PP03} (row 77) from Putirka et al. (2003) using *P* (kbar) by Putirka et al. (2003), $T_{P08\_Eq33\_PP03}$ (row 78) from Putirka (2008; Equation 33) using *P* (kbar) by Putirka et al. (2003), $T_{P08\_Eq33\_P1P96\_Iteratively}$ (row 79) from Putirka (2008; Equation 33) using *P*1(kbar) by Putirka et al. (1996), $T_{P08\_Eq33\_PNP17}$ (row 80) from Putirka (2008; Equation 33) using *P* (kbar) by Neave and Putirka (2017), $T_{P2M13\_Eq33\_P08}$ (row81) from Putirka (2008; Equation 33) using recalibrated *P*2 (kbar) by Masotta et al. (2013), $T_{P08\_Eq34\_PP03}$ (row 82) from Putirka (2008; Equation 34) using *P* (kbar) by Putirka et al. (2003), $T_{P08\_Eq34\_P1P96\_Iteratively}$ (row 83) from Putirka (2008; Equation 34) using *P*1 (kbar) by Putirka et al. (1996), T_{M13} (row 84) from Masotta et al. (2013); Input *P* (kbar) for hygrometer estimation (row 85), Input *T* (K) for hygrometer estimation (row 86), H_{A13} (row 87) from Armienti et al. (2013), H_{P16} (row 88) from Perinelli et al. (2016); D_{HZ87} (row 89) from Hill and Zucca (1987), D_{MT83_DBG11} (row 90) from Mavko and Thompson (1983) and DeBari and Greene (2011), D_{P09} (row 91) from Prezzi et al. (2009).

Orthopyroxene-liquid thermobarometers

Beattie (1993) developed an equation for the calculation of temperature based on orthopyroxene-liquid equilibria.

$$[T]^{opx-liq}_{B93}(\mathrm{K}) = \frac{\Delta H^{opx}_{M} / R + (P(\mathrm{GPa}) - 10^5) * \Delta V^{opx}_{M} / R}{\Delta S^{opx}_{M} / R + 2\ln D^{opx\text{-}L}_{M_*} + 2\ln C^{L}_{NM_*} - (NF)} \quad (1)$$

where ΔH, ΔS and ΔV are the enthalpy, entropy and volumes of fusion, *T* (K) and *P* (GPa) are the temperature and pressure, and *R* is the gas constant. In Eq. 1, M and the superscript L show the divalent cations (e.g. Mg, Fe, Mn, Ca) and melt phase (i.e. liquid), respectively. The $D^{Opx\text{-}L}_{M_*}$ and $C^{L}_{NM_*}$ components are estimated by using the empirical constants and thermodynamic parameters (in Table 1 and Table 2 by Beattie, 1993). The *NF* (network formers) component in Eq. 1 is the chemical constituents that consist of a silicate network in the liquid. This component is calculated from the *NF*=7/2*ln(1-$C^{L}_{AlO_{1.5}*}$)+7*ln(1-$C^{L}_{TiO_2*}$) equation, where all liquid components are based on cation fractions. Beattie's (1993) orthopyroxene-liquid thermometer estimation model by WinPLtb is listed in column number 197 both in the *Calculation Screen* window and an output Excel file (see row 58 in Table 4).

Although Beattie's (1993) model works well for some orthopyroxene-liquid compositions, Putirka (2008)

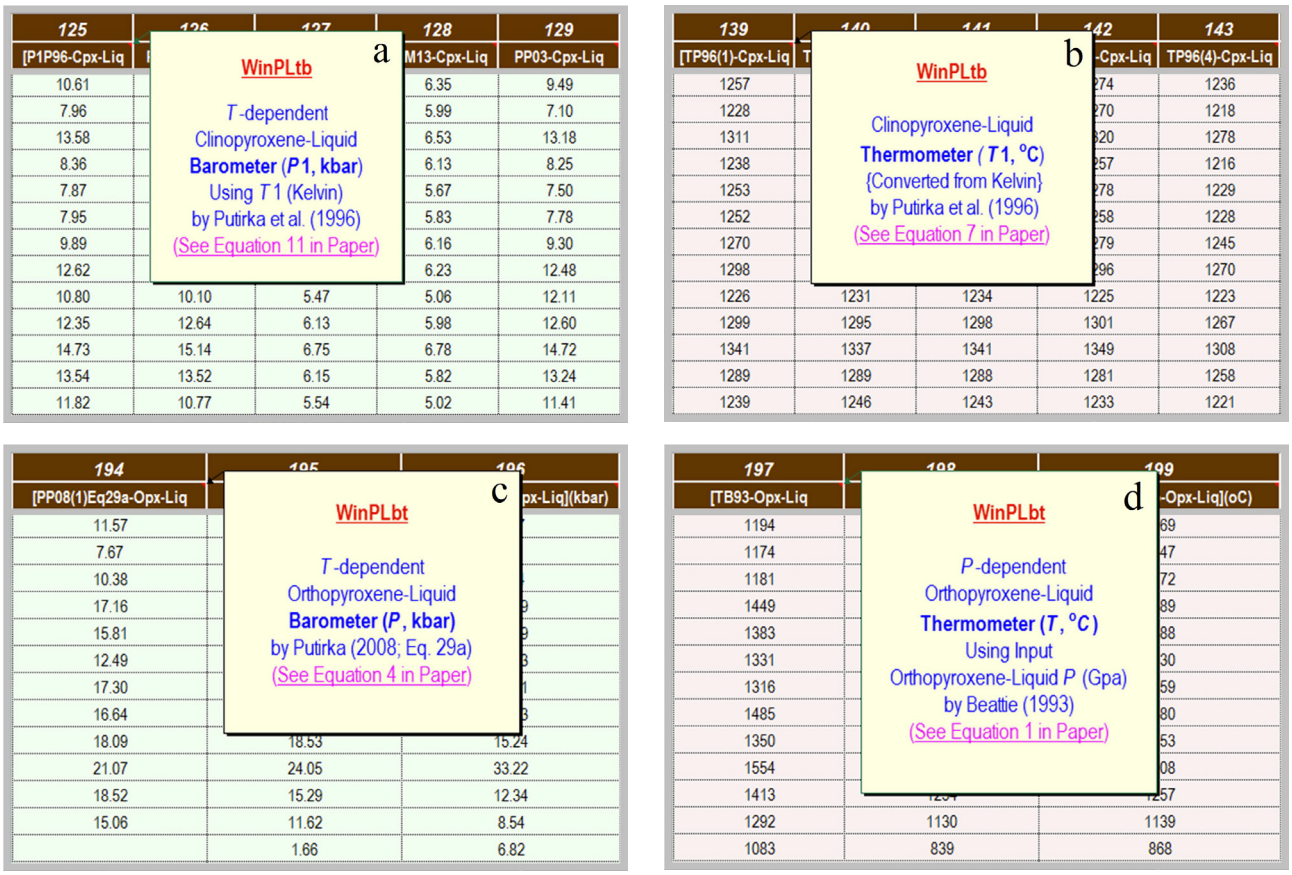

Figure 3. Screenshots of an output Excel (i.e. Output.xlsx) file along with explanations of (a) clinopyroxene-liquid barometers, (b) clinopyroxene-liquid thermometers, (c) orthopyroxene-liquid barometers, (d) orthopyroxene-liquid thermometers.

proposed two new thermometers for orthopyroxene-liquid (Eq. 2) and only-liquid (Eq. 3; to be used a liquid should become saturated with orthopyroxene) components to correct over estimations for hydrous and low estimations for some anhydrous compositions.

$$\frac{10^4}{[T1]^{opx-liq}_{P08\_Eq28a}(^{\circ}C)} = 4.07 - 0.329*[P(GPa)] + 0.12*[H_2O^{liq}]$$

$$+0.567*\ln\left[\frac{X^{opx}_{Fm_2Si_2O_6}}{(X^{liq}_{SiO_2})^2*(X^{liq}_{FeO}+X^{liq}_{MnO}+X^{liq}_{MgO})^2}\right] -3.06*[X^{liq}_{MgO}]$$

$$-6.17*[X^{liq}_{KO_{0.5}}] + 1.89*[Mg\#^{liq}] + 2.57*[X^{opx}_{Fe}] \qquad (2)$$

$$[T2]^{liq}_{P08\_Eq28b}(^{\circ}C) = \frac{5573.8 + 587.9*P(GPa) - 61*[P(GPa)]^2}{5.3 - 0.633*\ln(Mg\#^{liq}) - 3.97*(C^L_{NM}) + 0.06*}$$

$$\frac{5573.8 + 587.9*P(GPa) - 61*[P(GPa)]^2}{NF + 24.7*(X^{liq}_{CaO})^2 + 0.081*H_2O^{liq} + 0.156*P(GPa)} \qquad (3)$$

In these thermometers (see columns 198 and 199 in the *Calculation Screen* and rows 59 and 60 in Table 4), the term $X^{opx}_{Fm_2Si_2O_6}$ indicates the mole fraction of enstatite +ferrosilite (EnFs), C^L_{NM} shows the concentration of network modifying cations ($C^L_{NM}=X^{liq}_{MgO}+X^{liq}_{MnO}+X^{liq}_{FeO}+X^{liq}_{CaO}+X^{liq}_{NiO}$), and $Mg\#^{liq}$ states the magnesium number of cation fractions in liquid compositions [$Mg\#^{liq}=X^{liq}_{MgO}/(X^{liq}_{MgO}+X^{liq}_{FeO})$]. Comparison of orthopyroxene-liquid temperature estimations (i.e. Eqs. 2 and 3) by WinPLtb with an output by Putirka's (2018) Excel spreadsheet is shown in Figure 4a and Figure 4b, by applying the correlation coefficient and liner regression analysis techniques. It is evident that WinPLtb estimates the orthopyroxene-liquid temperature models by Putirka (2008) with high correlation coefficients. According to Putirka (2008), the range of applicability for orthopyroxene-liquid thermometer (Eq. 2), as well as only-liquid thermometer (Eq. 3), is T (°C)=750-1600 (±26 °C to±41 °C for the calibration data and test data, respectively), P (GPa)=0.0001-11.0, SiO_2 (wt%)=33-77 and H_2O (wt%)=0-14.2.

Using the $FmAl_2SiO_6$ and $NaAlSi_2O_6$ components of orthopyroxene compositions, as with the clinopyroxene equilibria, Putirka (2008) proposed two orthopyroxene-liquid (Eq. 4 and Eq. 5) and a single orthopyroxene barometers (Eq. 6).

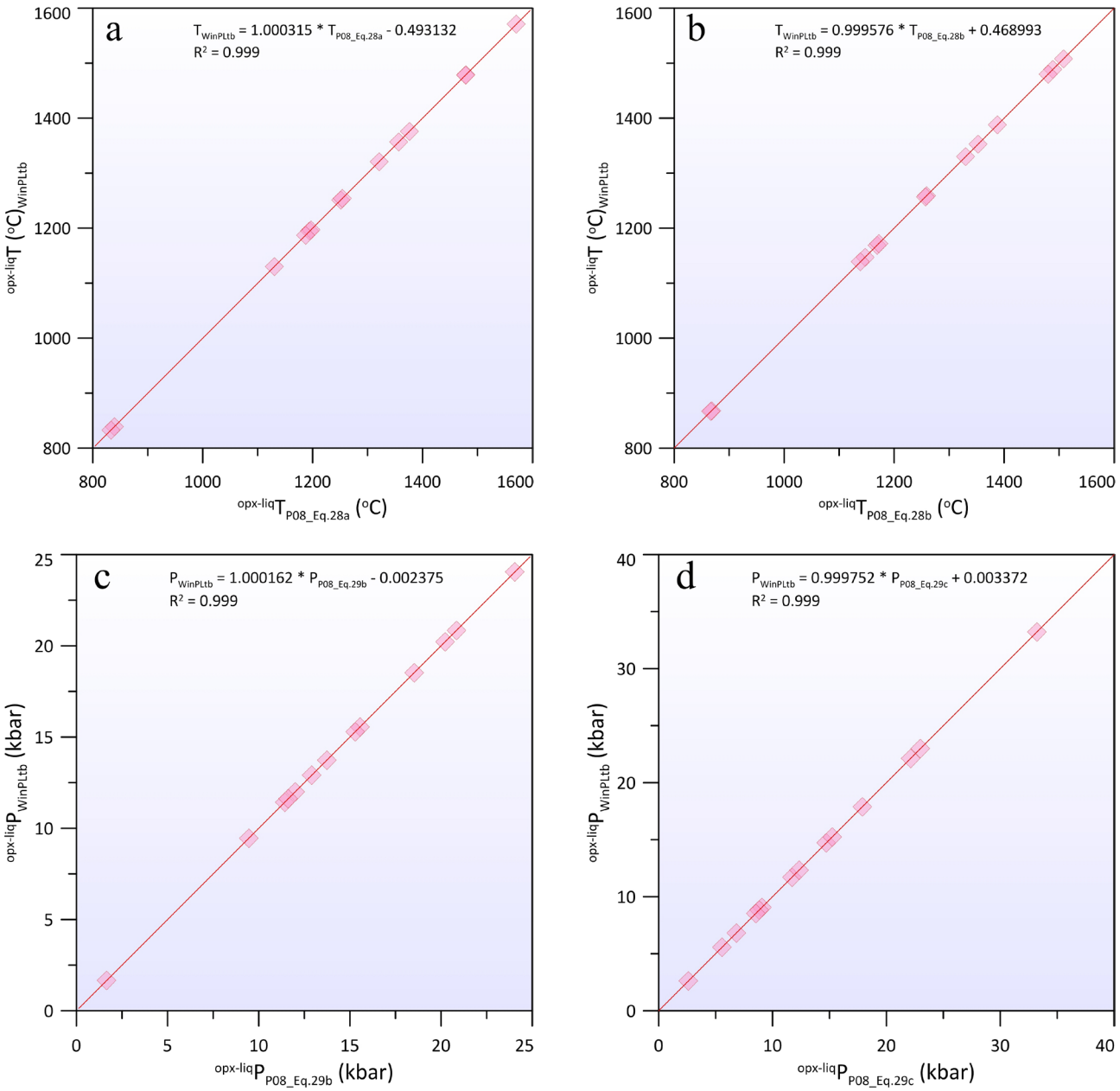

Figure 4. Comparison of orthopyroxene-liquid thermobarometers with an output by WinPLtb program for (a) Temperature estimation model by Putirka (2008; Eq. 28a), (b) Temperature estimation model by Putirka (2008; Eq. 28b), (c) Pressure estimation model by Putirka (2008; Eq. 29b), (d) Pressure estimation model by Putirka (2008; Eq. 29c). Data used in these figures are taken from Putirka (2018a).

$$[P]^{opx-liq}_{P08\_Eq29a}(\text{kbar}) = -13.97 + 0.0129*T(^{\circ}\text{C}) + 0.001416*$$
$$T(^{\circ}\text{C})*\ln\left[\frac{X^{opx}_{NaAlSi_2O_6}}{X^{liq}_{NaO_{0.5}} * X^{liq}_{AlO_{1.5}} * (X^{liq}_{SiO_2})^2}\right] - 19.64*(X^{liq}_{SiO_2}) +$$
$$47.49*(X^{liq}_{MgO}) + 6.99*(X^{opx}_{Fe}) + 37.37*(X^{opx}_{FmAl_2SiO_6})$$
$$+0.748*(H_2O^{liq}) + 79.67*(X^{liq}_{NaO_{0.5}} + X^{liq}_{KO_{0.5}}) \quad (4)$$

$$[P]^{opx-liq}_{P08\_Eq29b}(\text{kbar}) = 1.788 + 0.0375*T(^{\circ}\text{C}) + 1.295*10^{-3}*$$
$$T(^{\circ}\text{C})*\ln\left[\frac{X^{opx}_{FmAl_2SiO_6}}{X^{liq}_{FmO} * (X^{liq}_{AlO_{1.5}})^2 * X^{liq}_{SiO_2}}\right] - 33.42*(X^{liq}_{AlO_{1.5}})$$
$$+9.795*(Mg\#^{liq}) + 36.08*(X^{liq}_{NaO_{0.5}} + X^{liq}_{KO_{0.5}})$$
$$+0.784*(H_2O^{liq}) - 26.2*(X^{opx}_{Si}) + 14.21*(X^{opx}_{Fe}) \quad (5)$$

$$[P]^{opx}_{\text{P08\_Eq29c}}(\text{kbar}) = 2064 + 0.321*T(^{\circ}\text{C}) - 343.4*\ln*T(^{\circ}\text{C}) \cdot$$
$$+31.52*(X^{opx}_{\text{Al}}) - 12.28*(X^{opx}_{\text{Ca}}) - 290*(X^{opx}_{\text{Cr}}) \cdot$$
$$+1.54*\ln(X^{opx}_{\text{Cr}}) - 177.2*(X^{opx}_{\text{Al}} - 0.1715)^2$$
$$-372*(X^{opx}_{\text{Al}} - 0.1715)*(X^{opx}_{\text{Ca}} - 0.0736) \quad (6)$$

These barometers (see columns 194 to 196 in the *Calculation Screen* and rows 55 to 57 in Table 4) that based on the orthopyroxene-liquid equilibria were derived from global calibrations of nearly 600 experiments. The SEE of orthopyroxene-liquid barometers are low (± 2.6 kbar) when compared to the clinopyroxene-liquid models and these equations (Eq. 4 and Eq. 5) underestimate pressure at P > 30 kbar. According to Putirka (2008), Eq. 4 yields more accurate pressures for hydrous data (SEE±2.1 kbar) presumably reflecting more rapid orthopyroxene equilibration if H_2O is available in the system. Although orthopyroxene barometry model (Eq. 6) shows much less systematic error to 70 kbar for anhydrous data, the model exhibits high SEE (±4.1 kbar) for hydrous data. Similarly, comparison of pressure estimations (i.e. Eqs. 5 and 6) by WinPLtb with an output by Putirka's (2018a) Excel spreadsheet is shown in Figure 4c and Figure 4d with high correlation coefficients.

Clinopyroxene-liquid thermobarometers

Models for estimating the *P*-*T* conditions of igneous rocks from co-existing clinopyroxene and liquid components were calibrated by Putirka et al. (1996) based on existing and experimentally produced data on several mafic bulk compositions at 8-30 kbar and 1100-1475 °C. The jadeite (Jd)-diopside/hedenbergite (DiHd) exchange equilibrium between clinopyroxene and liquid is temperature sensitive and proposed *T*1 thermometer (see Figure 5a) estimates temperature to ± 27 K.

$$\frac{10^4}{[T1]^{cpx-liq}_{\text{P96}}(\text{K})} = 6.73 - 0.26*\ln\left[\frac{\text{Jd}^{cpx}*\text{Ca}^{liq}*\text{Fm}^{liq}}{\text{DiHd}^{cpx}*\text{Na}^{liq}*\text{Al}^{liq}}\right]$$
$$-0.86*\ln\left[\frac{\text{Mg}^{liq}}{\text{Mg}^{liq}+\text{Fe}^{liq}}\right] + 0.52*\ln\left[\text{Ca}^{liq}\right] \quad (7)$$

Similar approach on clinopyroxene-liquid equilibria resulting in *T*2 thermometer (see Figure 5b) which reduces the standard error estimate (SEE) from 27 to 24 K, but requires an empirical pressure (kbar) value as an input in temperature estimation.

$$\frac{10^4}{[T2]^{cpx-liq}_{\text{P96}}(\text{K})} = 6.59 - 0.16*\ln\left[\frac{\text{Jd}^{cpx}*\text{Ca}^{liq}*\text{Fm}^{liq}}{\text{DiHd}^{cpx}*\text{Na}^{liq}*\text{Al}^{liq}}\right] \quad (8)$$
$$-0.65*\ln\left[\frac{\text{Mg}^{liq}}{\text{Mg}^{liq}+\text{Fe}^{liq}}\right] + 0.23*\ln\left[\text{Ca}^{liq}\right] - 0.02*P(\text{kbar})$$

Putirka et al. (1996) also proposed two another clinopyroxene-liquid thermometers, *T*3 and *T*4, based on the calibration of DiHd-CaTs equilibrium.

$$\frac{10^4}{[T3]^{cpx-liq}_{\text{P96}}(\text{K})} = 6.92 - 0.18*\ln\left[\frac{\text{CaTs}^{cpx}*\text{Si}^{liq}*\text{Fm}^{liq}}{\text{DiHd}^{cpx}*\left[\text{Al}^{liq}\right]^2}\right]$$
$$-0.84*\ln\left[\frac{\text{Mg}^{liq}}{\text{Mg}^{liq}+\text{Fe}^{liq}}\right] - 0.29*\ln\left[\frac{1}{\left[\text{Al}^{liq}\right]^2}\right] \quad (9)$$

$$\frac{10^4}{[T4]^{cpx-liq}_{\text{P96}}(\text{K})} = 7.20 - 0.04*\ln\left[\frac{\text{CaTs}^{cpx}*\text{Si}^{liq}*\text{Fm}^{liq}}{\text{DiHd}^{cpx}*\left[\text{Al}^{liq}\right]^2}\right] \quad (10)$$
$$-0.59*\ln\left[\frac{\text{Mg}^{liq}}{\text{Mg}^{liq}+\text{Fe}^{liq}}\right] - 0.18*\ln\left[\frac{1}{\left[\text{Al}^{liq}\right]^2}\right] - 0.03*P(\text{kbar})$$

In these equations (see columns 139 to 143 in the *Calculation Screen* and rows 67 to 71 in Table 5), the terms Jd^{cpx}, DiHd^{cpx} and CaTs^{cpx} show the mole fractions of jadeite, diopside+hedenbergite and calcium tschermak's components, X^i_j denotes the cation fraction of *i* in phase *j*, and Fm^{liq} indicates the sum MgO^{liq}+FeO^{liq}. Putirka et al. (1996) stated that models *T*1 and *T*2 which using the DiHd-Jd components are somewhat better than models *T*3 and *T*4 with the DiHd-CaTs components based on regression analysis and statistical evaluations. Calculated SEEs for the pressure-independent (*T*1 and *T*3) and pressure-dependent (*T*2 and *T*4) models are 40 K and 30 K, respectively. Hence, temperature estimations based on the pressure-dependent models (*T*2 and *T*4) may show slightly more accurate results when compared to the pressure-independent (*T*1 and *T*3) models.

The Jd-liq equilibrium, which has a high ΔV_r, is considered as a useful barometer. Compared to the Jd-DiHd exchange equilibrium between clinopyroxene and liquid, the equilibrium constant for jadeite formation is more sensitive to pressure, thus resulting in a temperature-dependent barometers (Putirka et al., 1996; see columns 125 and 126 in the *Calculation Screen* and rows 53 and 54 in Table 5).

$$[P1]^{cpx-liq}_{\text{P96}}(\text{kbar}) = -54.3 + 299*\frac{T(\text{K})}{10^4} + 36.4*\frac{T(\text{K})}{10^4}*$$
$$\ln\left[\frac{\text{Jd}^{cpx}}{[\text{Si}^{liq}]^2*\text{Na}^{liq}*\text{Al}^{liq}}\right] + 367*\left[\text{Na}^{liq}*\text{Al}^{liq}\right] \quad (11)$$

$$[P2]^{cpx-liq}_{\text{P96}}(\text{kbar}) = -50.7 + 394*\frac{T(\text{K})}{10^4} + 36.4*\frac{T(\text{K})}{10^4}* \quad (12)$$
$$\ln\left[\frac{Jd^{cpx}}{[\text{Si}^{liq}]^2*\text{Na}^{liq}*\text{Al}^{liq}}\right] - 20.0*\frac{T(\text{K})}{10^4}*\ln\left[\frac{1}{\text{Na}^{liq}*\text{Al}^{liq}}\right]$$

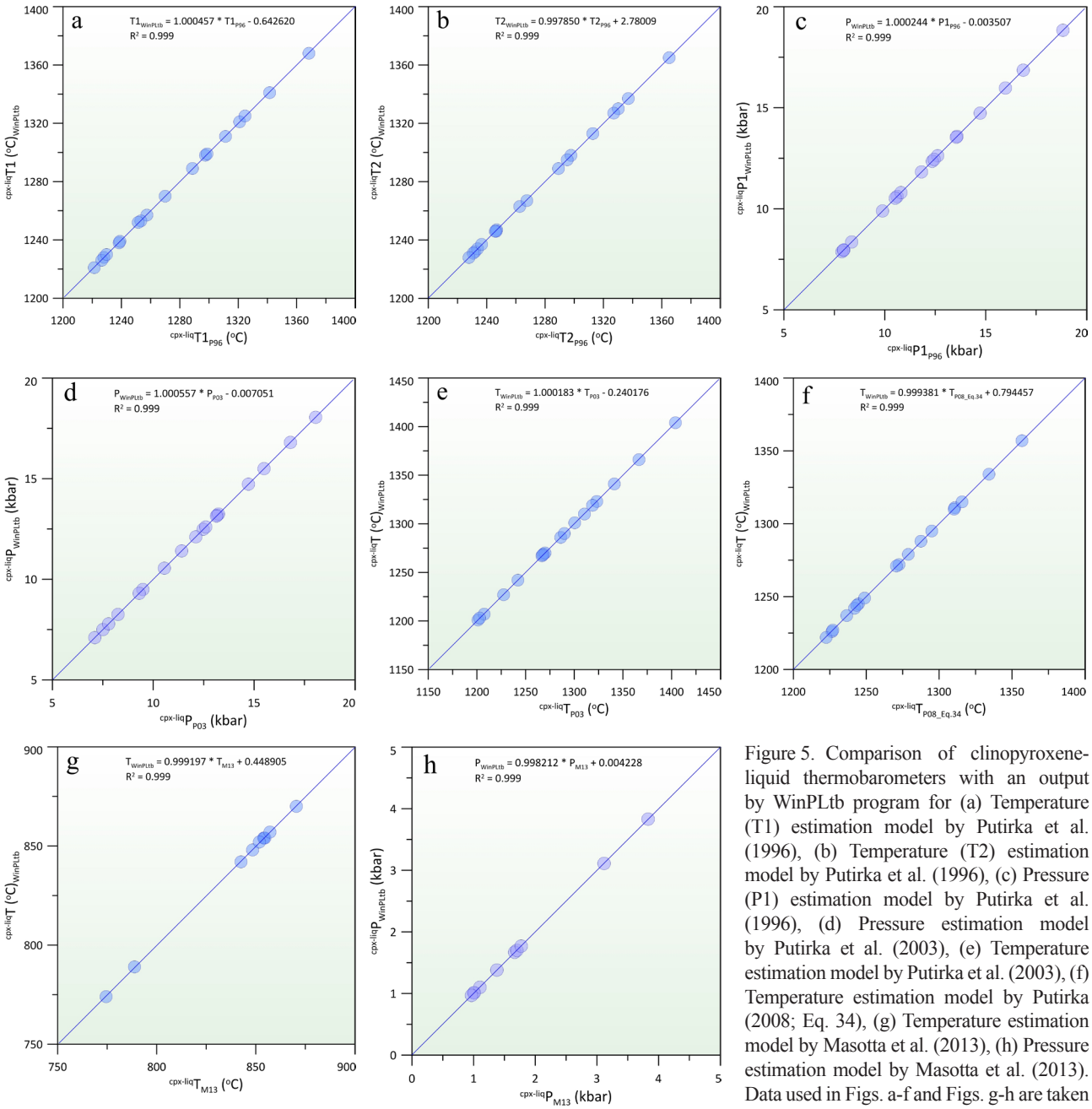

Figure 5. Comparison of clinopyroxene-liquid thermobarometers with an output by WinPLtb program for (a) Temperature (T1) estimation model by Putirka et al. (1996), (b) Temperature (T2) estimation model by Putirka et al. (1996), (c) Pressure (P1) estimation model by Putirka et al. (1996), (d) Pressure estimation model by Putirka et al. (2003), (e) Temperature estimation model by Putirka et al. (2003), (f) Temperature estimation model by Putirka (2008; Eq. 34), (g) Temperature estimation model by Masotta et al. (2013), (h) Pressure estimation model by Masotta et al. (2013). Data used in Figs. a-f and Figs. g-h are taken from Putirka (2018b) and Masotta et al. (2013), respectively.

According to Putirka et al. (1996), *P*1 model (see Figure 5c) that calculates pressure to ±1.4 kbar represents compositional dependencies in their empirical form, while *P*2 model uses the explicit activity-modifying form. In comparison of models on the basis of regression analysis and statistics, *P*1 model has been proposed by Putirka et al. (1996) in clinopyroxene-liquid pressure estimation due to the lowest SEE.

Considering most of clinopyroxene-liquid thermobarometers have been calibrated from basaltic liquid compositions, Putirka et al. (2003) suggested new thermobarometers (see Fig. 5 d,e) using new experiments that contain hydrated and SiO_2-rich liquids.

$$[P]_{P03}^{cpx-liq}(\text{kbar}) = -88.3 + 2.82*10^{-3}*T(\text{K})* \ln\left[\frac{\left[\text{Jd}^{cpx}\right]}{\text{Na}^{liq}*\text{Al}^{liq}*\left[\text{Si}^{liq}\right]^2}\right] + 2.19*10^{-2}*T(\text{K}) - 25.1*$$

$$\ln\left[Ca^{liq}*Si^{liq}\right]+7.03*\left[Mg^{liq}\right]+12.4*\ln\left[Ca^{liq}\right] \quad (13)$$

$$\frac{10^4}{[T]^{cpx-liq}_{P03}(K)}=4.60-4.37*10^{-1}*\ln\left[\frac{\left[Jd^{cpx}*Ca^{liq}*Fm^{liq}\right]}{\left[DiHd^{cpx}*Na^{liq}*Al^{liq}\right]}\right]-6.54*10^{-1}*\ln\left[Mg^{liq}\right]-3.26*10^{-1}*\ln\left[Na^{liq}\right]-6.32*10^{-3}*\left[P(kbar)\right]-0.92*\ln\left[Si^{liq}\right]+2.74*10^{-1}*\ln\left[Jd^{liq}\right] \quad (14)$$

The SEEs for proposed barometer (see columns 129 and 130 in the *Calculation Screen* and rows 57 and 58 in Table 5) and thermometer (see column 149 in the *Calculation Screen* and row 77 in Table 5) are 1.7 kbar and 33 K, respectively. Although these thermobarometers seem more complex when compared to the models by Putirka et al. (1996), they estimate the *P-T* conditions successfully for a wide range of rock compositions.

To better define hydrous samples, Putirka (2008) calibrated previous clinopyroxene-liquid barometers (e.g. Putirka et al., 1996, 2003) using the H_2O (wt%) content in liquid as an input variable in the following equations (see columns 131 and 132 in the *Calculation Screen* and rows 59 and 60 in Table 5).

$$[P]^{cpx-liq}_{P08\_Eq30}(kbar)=-48.7+271*\frac{T(K)}{10^4}+32*\frac{T(K)}{10^4}*\ln\left[\frac{X^{cpx}_{NaAlSi_2O_6}}{X^{liq}_{NaO_{0.5}}*X^{liq}_{AlO_{1.5}}*(X^{liq}_{SiO_2})^2}\right]-8.2*\ln(X^{liq}_{FeO})+4.6*\ln(X^{liq}_{MgO})-0.96*(X^{liq}_{KO_{0.5}})-2.2*\ln(X^{cpx}_{DiHd})-31*(Mg\#^{liq})+56*(X^{liq}_{NaO_{0.5}}+X^{liq}_{KO_{0.5}})+0.76*(H_2O^{liq}) \quad (15)$$

$$[P]^{cpx-liq}_{P08\_Eq31}(kbar)=-40.73+358*\frac{T(K)}{10^4}+21.69*\frac{T(K)}{10^4}*\ln\left[\frac{X^{cpx}_{NaAlSi_2O_6}}{X^{liq}_{NaO_{0.5}}*X^{liq}_{AlO_{1.5}}*(X^{liq}_{SiO_2})^2}\right]-105.7*(X^{liq}_{CaO})-165.5*(X^{liq}_{NaO_{0.5}}+X^{liq}_{KO_{0.5}})^2-50.15*(X^{liq}_{SiO_2})*(X^{liq}_{FeO}+X^{liq}_{MgO})-3.178*\ln(X^{cpx}_{DiHd})-2.205*\ln(X^{cpx}_{EnFs})+0.864*\ln(X^{cpx}_{Al})+0.3962*(H_2O^{liq}) \quad (16)$$

To improve the precision of Nimis (1995) model with removing the systematic error, Putirka (2008) proposed a barometer (see column 133 in the *Calculation Screen* and rows 61 in Table 5) requiring an estimate of the H_2O (wt%) content of the liquid in equilibrium with the clinopyroxene composition and additional estimations for the fractions of Fe *(apfu)* and Mg *(apfu)* in the M1 and M2 sites.

$$[P]^{cpx-liq}_{P08\_Eq32b}(kbar)=1458+0.197*T(K)-241*\ln(T(K)+0.453*(H_2O^{liq})+55.5*(X^{cpx}_{Al^{VI}})+8.05*(X^{cpx}_{Fe})-277*(X^{cpx}_{K})+18*(X^{cpx}_{Jd})+44.1*(X^{cpx}_{DiHd})+2.2*\ln(X^{cpx}_{Jd})-27.7*(X^{cpx}_{Al})^2+97.3*(X^{cpx}_{Fe_{M2}})^2+30.7*(X^{cpx}_{Mg_{M2}})^2-27.6*(X^{cpx}_{DiHd})^2 \quad (17)$$

A new barometer (Eq. 18; see column 134 in the *Calculation Screen* and rows 62 in Table 5) based on the partitioning of Al contents between clinopyroxene and liquid is also developed by Putirka (2008) with the SEE = ± 1.5 kbar.

$$[P]^{cpx-liq}_{P08\_Eq32c}(kbar)=-57.9+0.0475*T(K)-40.6*(X^{liq}_{FeO})-47.7*(X^{cpx}_{CaTs})+0.67*(H_2O^{liq})-153*(X^{liq}_{CaO_{0.5}}*X^{liq}_{SiO_2})+6.89*\left[\frac{X^{cpx}_{Al}}{X^{liq}_{AlO_{1.5}}}\right] \quad (18)$$

Putirka (2008) reported that the previous Jd-DiHd exchange clinopyroxene-liquid thermometers (i.e. Putirka et al., 1996; 2003) reproduce temperature to ± 52-60 °C, but uncertainties at these thermometers were reduced to 10-20 °C by using the global calibrations for experiments conducted at P<70 kbar (see columns 150 to 155 in the *Calculation Screen* and rows 78 to 82 in Table 5 for different pressure values).

$$\frac{10^4}{[T]^{cpx-liq}_{P08\_Eq33}(K)}=7.53-0.14*\ln\left[\frac{X^{cpx}_{Jd}*X^{cliq}_{CaO}*X^{liq}_{Fm}}{X^{cpx}_{DiHd}*X^{liq}_{Na}*X^{liq}_{Al}}\right]+0.07*(H_2O^{liq})-14.9*(X^{liq}_{CaO}*X^{liq}_{SiO_2})-0.08*\ln(X^{liq}_{TiO_2})-3.62*(X^{liq}_{NaO_{0.5}}+X^{liq}_{KO_{0.5}})-1.1*(Mg\#^{liq})-0.18*\ln(X^{cpx}_{EnFs})-0.027*P(kbar) \quad (19)$$

$$\frac{10^4}{[T]^{liq}_{P08\_Eq34}(K)}=6.39+0.076*(H_2O^{liq})-5.55*(X^{liq}_{CaO}*X^{liq}_{SiO_2})-0.386*\ln(X^{liq}_{MgO})-0.04*P(kbar)+2.2*10^{-4}*\left[P(kbar)\right]^2 \quad (20)$$

Temperature estimation (see Figure 5f), which is based on a liquid saturated with clinopyroxene composition (i.e. Eq. 20) can be used to test the calibrations (e.g. Eq. 19) derived from clinopyroxene-liquid equilibria (Putirka, 2008).

Masotta et al. (2013) proposed a new thermometer (Eq. 21; see column 156 in the *Calculation Screen* and rows 73 in Table 5) and barometer (Eq. 22; see column 136 in the *Calculation Screen* and rows 84 in Table 5) based on clinopyroxene-liquid equilibria that were calibrated by using regression analyses of experimental dataset from literature and new experiments for alkaline differentiated

magmas with clinopyroxene-bearing trachytic and phonolitic melt compositions (i.e. SiO_2=53-69 wt% and Na_2O+K_2O=10-17 wt%), equilibrated at 700-1000 °C and 0.5-3.0 kbar conditions.

$$\frac{10^4}{[T]^{cpx-liq}_{M13}(K)} = 2.91 - 0.4*\ln\left[\frac{\left(X^{cpx}_{Jd}*X^{liq}_{Ca}*X^{liq}_{Fm}\right)}{\left(X^{cpx}_{DiHd}*X^{liq}_{Na}*X^{liq}_{Al}\right)}\right] + 0.038*$$
$$(H_2O^{liq}) - 1.64*\left[\frac{\left(\frac{X^{liq}_{Mg}}{X^{liq}_{Mg}+X^{liq}_{Fe}}\right)}{\left(X^{cpx}_{DiHd}\right)}\right] + 1.01*\left[\frac{X^{liq}_{Na}}{\left(X^{liq}_{Na}+X^{liq}_{K}\right)}\right] - 0.22*$$
$$\ln\left(X^{liq}_{Ti}\right) + 0.47*\ln\left[\frac{X^{cpx}_{Jd}}{\left(X^{liq}_{Na}*X^{liq}_{Al}\right)*\left(X^{liq}_{Si}\right)^2}\right] + 1.62*\left(K^{cpx-liq}_{D(Fe-Mg)}\right)$$
$$+ 23.39*\left(X^{liq}_{Ca}*X^{liq}_{Si}\right) \quad (21)$$

$$[P]^{cpx-liq}_{M13}(kbar) = -3.89 + 0.28*\left[\frac{X^{cpx}_{Jd}}{\left(X^{liq}_{Na}*X^{liq}_{Al}\right)*\left(X^{liq}_{Si}\right)^2}\right] + 0.074*\left(H_2O^{liq}\right) + 5.01*\left(\frac{X^{liq}_{Na}}{\left(X^{liq}_{Na}+X^{liq}_{K}\right)}\right) + 6.39*\left(K^{cpx-liq}_{D(Fe-Mg)}\right) \quad (22)$$

In these equations, the terms $K^{Cpx\text{-}liq}_{D(Fe\text{-}Mg)}$ and $X^{liq}_{Na}/(X^{liq}_{Na}+X^{liq}_{K})$ show the Fe-Mg exchange based on molar ratio of $(Fe/Mg)^{cpx}/(Fe/Mg)^{liq}$ and Na-*number* (i.e. $Na\#^{liq}$), respectively. The use of these terms in the temperature estimation has improved the precision from SEE_T=18.2 °C to about 6-15 °C with respect to the standard error of estimate of recalibrated equations. According to Masotta et al. (2013), the new thermometer (see Figure 5g) and barometer (see Figure 5h) can be used reliably to estimate the magmatic *P-T* conditions in alkaline magma reservoirs feeding highly explosive eruptions.

Masotta et al. (2013) also recalibrated previous clinopyroxene-liquid models developed by Putirka et al. (1996) for *T*1 to *T*4 (see Eq. 23 to 26; see columns 145 and 148 in the *Calculation Screen* and rows 73 and 76 in Table 5) and *P*1 and *P*2 (see Eq. 27 and Eq. 28; see columns 127 and 128 in the *Calculation Screen* and rows 55 and 56 in Table 5) and by Putirka (2008) for Eq. 32c (see Eq. 29; see column 135 in the *Calculation Screen* and row 63 in Table 5) and Eq. 33 (see Eq. 30; see column 153 in the *Calculation Screen* and row 81 in Table 5), because of their common applications to volcanogenic studies and their calibrations at *P-T* conditions including a typical of alkaline differentiated magma suit (e.g. Mollo et al., 2010 a,b).

$$\frac{10^4}{[T1]^{cpx-liq}_{M13\_P96}(K)} = 6.7423 - 0.0232*\ln\left[\frac{Jd^{cpx}*Ca^{liq}*Fm^{liq}}{DiHd^{cpx}*Na^{liq}*Al^{liq}}\right]$$
$$- 0.6884*\ln\left[\frac{Mg^{liq}}{Mg^{liq}+Fe^{liq}}\right] - 0.1532*\ln\left[Ca^{liq}\right] \quad (23)$$

$$\frac{10^4}{[T2]^{cpx-liq}_{M13\_P96}(K)} = 6.5239 - 0.0396*\ln\left[\frac{Jd^{cpx}*Ca^{liq}*Fm^{liq}}{DiHd^{cpx}*Na^{liq}*Al^{liq}}\right]$$
$$- 0.6806*\ln\left[\frac{Mg^{liq}}{Mg^{liq}+Fe^{liq}}\right] - 0.1457*\ln\left[Ca^{liq}\right] + 0.0791*P(kbar) \quad (24)$$

$$\frac{10^4}{[T3]^{cpx-liq}_{M13\_P96}(K)} = 5.0528 - 0.0569*\ln\left[\frac{CaTs^{cpx}*Si^{liq}*Fm^{liq}}{DiHd^{cpx}*\left[Al^{liq}\right]^2}\right]$$
$$- 0.8124*\ln\left[\frac{Mg^{liq}}{Mg^{liq}+Fe^{liq}}\right] + 0.679*\ln\left[\frac{1}{\left[Al^{liq}\right]^2}\right] \quad (25)$$

$$\frac{10^4}{[T4]^{cpx-liq}_{M13\_P96}(K)} = 3.8541 - 0.0632*\ln\left[\frac{CaTs^{cpx}*Si^{liq}*Fm^{liq}}{DiHd^{cpx}*\left[Al^{liq}\right]^2}\right]$$
$$- 0.8724*\ln\left[\frac{Mg^{liq}}{Mg^{liq}+Fe^{liq}}\right] + 0.9056*\ln\left[\frac{1}{\left[Al^{liq}\right]^2}\right] + 0.1861*P(kbar) \quad (26)$$

$$[P1]^{cpx-liq}_{M13\_P96}(kbar) = -8.8337 + 79.0497*\frac{T(K)}{10^4} + 11.6474*\frac{T(K)}{10^4}*\ln\left[\frac{Jd^{cpx}}{[Si^{liq}]^2*Na^{liq}*Al^{liq}}\right] + 8.6331*\left[Na^{liq}*Al^{liq}\right] \quad (27)$$

$$[P2]^{cpx-liq}_{M13\_P96}(kbar) = -6.2833 + 38.1796*\frac{T(K)}{10^4} + 9.4211*\frac{T(K)}{10^4}*\ln\left[\frac{Jd^{cpx}}{[Si^{liq}]^2*Na^{liq}*Al^{liq}}\right] + 6.1564*\frac{T(K)}{10^4}*\ln\left[\frac{1}{Na^{liq}*Al^{liq}}\right] \quad (28)$$

$$[P]^{cpx-liq}_{M13\_P08\_Eq32c}(kbar) = -16.3446 + 0.0141*T(K) - 12.3909*(X^{liq}_{FeO}) - 9.1922*(X^{cpx}_{CaTs}) + 0.214*(H_2O^{liq}) + 38.734*(X^{liq}_{CaO_{0.5}}*X^{liq}_{SiO_2}) + 1.5944*\left[\frac{X^{cpx}_{Al}}{X^{liq}_{AlO_{1.5}}}\right] \quad (29)$$

$$\frac{10^4}{[T]^{cpx-liq}_{M13\_P08\_Eq33}(K)} = 6.8073 + 0.0027*\ln\left[\frac{X^{cpx}_{Jd}*X^{cliq}_{CaO}*X^{liq}_{Fm}}{X^{cpx}_{DiHd}*X^{liq}_{Na}*X^{liq}_{Al}}\right] + 0.0501*(H_2O^{liq}) - 25.0429*(X^{liq}_{CaO}*X^{liq}_{SiO_2}) - 0.3042*\ln(X^{liq}_{TiO_2}) + 2.2544*(X^{liq}_{NaO_{0.5}}+X^{liq}_{KO_{0.5}}) - 1.9145*(Mg\#^{liq}) - 0.0211*\ln(X^{cpx}_{EnFs}) + 0.0615*P(kbar) \quad (30)$$

According to Masotta et al. (2013), the recalibrated equations *T*1 and *T*2 (i.e. Eq. 23 and Eq. 24) show much

lower errors than those from the original equations developed by Putirka et al. (1996) with the SSE_{T1}=31.6 ºC and SSE_{T2}=31.2 ºC, respectively. On the other hand, the recalibrated temperature estimation (i.e. Eq. 30) by Masotta et al. (2013) based on clinopyroxene-liquid equilibria gives the best precision (SEE_{T33}=24.0 ºC) when compared their other recalibrated temperature equations (i.e. Eqs. 23 to 26). Masotta et al. (2013) pointed out that due to relatively narrow pressure range of the experimental dataset between 0.5 and 3.0 kbar, the recalibration of the pressure estimations did not show an improved precision. However, using additional clinopyroxene-liquid pairs for peralkaline rocks, as well as basaltic to rhyolitic rocks with both alkaline and sub-alkaline affinity from the Library of Experimental Phase Relations (LEPR) dataset, they significantly improved the precision of previous clinopyroxene-liquid barometers developed by Putirka et al. (1996) and Putirka (2008). Their recalibrated pressure equations (i.e. Eq. 27 and Eq. 28) give two to five times lower SSE than those of Putirka et al.'s (1996) models (SSE_{P1}=1.71 kbar; SSE_{P2}=1.70 kbar) and a better SEE_P=1.67 kbar (see Eq. 29) for Putirka's (2008) model (i.e. Eq. 32c), which is based on the partitioning of Al between clinopyroxene and liquid equilibria.

Taking into account some inaccuracies on commonly used clinopyroxene-liquid barometers with data from experiments on H_2O-poor tholeiites in the range of 1 atm to 10 kbar, Neave and Putirka (2017) proposed a new barometer that was calibrated from experimental data in the 1 atm to 20 kbar range to improve the accuracy of Jd-in-clinopyroxene barometry.

$$[P]^{cpx-liq}_{\mathrm{NP17}}(\mathrm{kbar}) = -26.27 + 39.16 * \frac{T(\mathrm{K})}{10^4} * \ln\left[\frac{X^{cpx}_{\mathrm{Jd}}}{X^{liq}_{\mathrm{NaO_{0.5}}} * X^{liq}_{\mathrm{AlO_{1.5}}} * \left(X^{liq}_{\mathrm{SiO_2}}\right)^2}\right] - 4.22 * \ln\left(X^{cpx}_{\mathrm{DiHd}}\right) + 78.43 * X^{liq}_{\mathrm{AlO_{1.5}}} + 393.81 * \left(X^{liq}_{\mathrm{NaO_{0.5}}} * X^{liq}_{\mathrm{KO_{0.5}}}\right)^2 \quad (31)$$

This clinopyroxene-liquid barometer (see columns 137 and 138 in the *Calculation Screen* and rows 65 and 66 in Table 5), with a SEE of ±1.4 kbar, can be used for hydrous and anhydrous samples from ultramafic to intermediate in compositions. However, Neave and Putirka (2017) advised to use clinopyroxene-liquid barometry with caution below 1100 ºC and at oxygen fugacities greater than one log unit above the quartz-fayalite-magnetite (QFM) buffer conditions. According to Neave and Putirka (2017), current barometer offers a significant improvement in accuracy when compared to previous versions of clinopyroxene-liquid barometers.

Clinopyroxene-based hygrometers and depth estimations

Magma transport and storage conditions are necessary criteria for the history of magma evolution, crystallization, and eruption processes. Of the storage conditions, pressure can effect main aspects of magma crystallization period and, thus plays an important role in understanding the crustal conditions where the magmas evolve (Harmon et al., 2018). Pressures of crystallization, for instance, estimated from pyroxene-liquid thermobarometers can be translated into magma staging depths and then used to constrain the magma transport and storage conditions (Putirka, 1997). WinPLtb estimates three magma depths (km) using the pressure (kbar) obtained from clinopyroxene-liquid barometer for the density model of Hill and Zucca (1987; see Eq. 32) and density-depth models by Mavko and Thompson (1983) and DeBari and Greene (2011; see Eq. 33) and Prezzi et al. (2009; see Eq. 34).

$$D_{\mathrm{HZ87\_PNP17}}(\mathrm{km}) = -2.77*10^{-5}*[P^4(\mathrm{kbar})] - 2.0*10^{-3}*[P^3(\mathrm{kbar})] - 4.88*10^{-2}*[P^2(\mathrm{kbar})] + 3.6*P(\mathrm{kbar}) - 6.34*10^{-2} \quad (32)$$

$$D_{\mathrm{MT83\&DG11\_PNP17}}(\mathrm{km}) = -2.4*10^{-4}*[P^3(\mathrm{kbar})] - 2.11*10^{-2}*[P^2(\mathrm{kbar})] + 3.6*P(\mathrm{kbar}) + 0.46 \quad (33)$$

$$D_{\mathrm{P09\_PNP17}}(\mathrm{km}) = 4.88 + 3.30*P(\mathrm{kbar}) - 0.0137*[P(\mathrm{kbar}) - 18.01]^2 \quad (34)$$

The program calculates magma depths (km) using the input *P* (kbar) typed in the *Data Entry Screen*, from clinopyroxene-liquid barometers developed by Putirka et al. (2003; see Eq. 13), Putirka (2008; see Eq. 15) and Masotta et al. (2013; see Eq. 22) if one of these options is selected from the *Depths* menu in the *Start-up* or *Data Entry Screen* and lists them (see rows 89 to 91 in Table 5) between columns 158 and 160 in the *Calculation Screen* and an Excel output file.

Although volatiles are only present in small amounts in magmas, their influence is great for the volcanic eruptions. The solubility of volatile species (e.g. H_2O, CO_2, S, Cl, and F) in magmas is a pressure-sensitive phenomenon that affects the compositional range of the gas phase as a function of depth and magma degassing process (Armienti et al., 2013). Hence, the presence of dissolved volatiles, especially H_2O and to a lesser extent CO_2, in silicate melts controls the density, as well as the abundance and composition of crystal phases in magma during cooling and decompression (Edmonds and Wallace, 2017). Armienti et al. (2013) investigated the deep portion of the Mt. Etna magma feeding environment and proposed a method to estimate the magma ascent rates at greater depths of a volcano plumbing system. Their approach is essentially based on the calculation of *P-T* conditions of Mt. Etna

magmas using clinopyroxene-liquid thermobarometry by Putirka et al. (2003) and developing an empirical hygrometer for Mt. Etna lavas to estimate the water contents (H_2O wt%) obtained from clinopyroxene compositions.

$$H_2O_{A13}\ (wt\%) = \frac{19.45*DiHd - 0.62*EnFs + 8.39*CaTs}{3.92} + \frac{+ 49.33*Jd - 86.02*CaTi - 0.37*P\ (GPa) - 0.37*T^{-1}(^oC)}{3.92} \quad (35)$$

According to Armienti et al. (2013), the presented empirical hygrometer recovers water contents of the calibrating experiments with low SEE of ±0.5 wt% and is restricted only to clinopyroxenes in equilibrium with trachybasaltic and hawaiitic melts. Their model works for the P-T-H_2O-CO_2 path of fluid-undersaturated magmas feeding some important eruptions having the clinopyroxene liquids that constrained within the 500-900 MPa, 1100-1180 ^oC, 3-4 %wt H_2O, and 0.23-0.31 wt% CO_2 ranges.

Because Eq. 35 does not successfully predict the melt-H_2O content in equilibrium with clinopyroxenes from Etnean trachybasalts, Perinelli et al. (2016) proposed a new hygrometer to improve the ability to predict water contents for a broader range of melt and clinopyroxene compositions.

$$H_2O_{P16}(wt\%)=39.60*DiHd+29.48*EnFs+41.76*CaTs+39.58*Jd+0.44*CaTi+0.14*\ln P(MPa)-0.01*T(°C)-27.53 \quad (36)$$

Clinopyroxenes used in the Perinelli et al. (2016) model were equilibrated upon H_2O-undersaturated and H_2O-saturated conditions with Etnean melts consist of basalt, trachybasalt, and basaltic trachyandesite compositions containing water contents within the range of 1-5 wt% and experimental conditions at P (MPa)=27-800, T (^oC)=1000-1175, and fO_2=QFM (quartz-fayalite-magnetite)-NNO+2 (nickel-nickel oxide) buffers. WinPLtb calculates two hygrometers (wt%) using the pressure (kbar) and temperature (K) values obtained from clinopyroxene-liquid thermobarometer. The program estimates hygrometers (wt%) using the input P (kbar) and T (K) values entered in the *Data Entry Screen*, from clinopyroxene-liquid thermobarometers developed by Putirka (2008; see Eq. 15 and Eq. 19), Putirka (2008; see Eq. 15) and Masotta et al. (2013; see Eq. 21 and Eq. 22) if one of these options is selected from the *Hygrometers* menu in the *Start-up* or *Data Entry Screen* and lists them (see rows 87 and 88 in Table 5) in columns 162 and 163 in the *Calculation Screen* and an Excel output file.

SUMMARY AND AVAILABILITY OF THE PROGRAM

WinPLtb is developed for personal computers running in the Windows operating system to estimate the P-T conditions of pyroxene-bearing rocks based on pyroxene-liquid equilibria. The program calculates multiple clino- and orthopyroxene analyses on the basis of six oxygens, obtained both from wet-chemical and electron-microprobe techniques, using different normalizations (e.g. structural formulae with/without total four cations) and ferric iron (e.g. Droop, 1987; Papike et al., 1974) estimation methods.

The program generates two main windows. The first window (i.e. *Start-up/New File*/*Data Entry Screen*) appears on the screen with several pull-down menus and equivalent shortcuts. By selecting options or clicking buttons on the *Start-up* screen, the user can enter new or load previously typed pyroxene and liquid analyses into the data entry section for a desired calculation scheme. Mainly four group analyses including clinopyroxene, orthopyroxene and liquid compositions equilibrated with clino- and orthopyroxenes can be entered in a new file with variables highlighted by light cyan, light green, faded pink and light yellow colors. The last three columns (i.e. P(GPa)$^{[lopyx]}$, T(K)$^{[lcpyx]}$, P(kbar)$^{[lcpyx]}$) with edited P-T data in the *New File*/*Data Entry Screen*, enable to estimate the P-dependent orthopyroxene-liquid thermometers as well as the T- and P-dependent clinopyroxene-liquid thermobarometers by selecting the second and third options from the pull-down menu of *Thermobarometers*. WinPLtb also calculates clinopyroxene-based depths (km) and clinopyroxene-liquid hygrometers (wt%) for different P (kbar) and P-T (kbar, K) values by selecting options from the pull-down menu of *Depths* and *Hygrometers* in the *Data Entry Screen*, respectively. By clicking the *Calculate* icon (i.e. ∑) in the *Data Entry Screen*, all calculated parameters by program are transferred to the second window (i.e. *Calculation Screen*).

The second window (i.e. *Calculation Screen*) allows the user to display these parameters on screen including major oxide pyroxene and liquid compositions (wt%), recalculated cations *(apfu)* of pyroxene analyses, clino- and orthopyroxene components, liquid cation fractions equilibrated with clino- and orthopyroxenes, clinopyroxene-liquid and orthopyroxene-liquid thermobarometers (^oC, kbar), depth (km) values based on clinopyroxene-liquid barometer, and clinopyroxene-based hygrometers (wt%). WinPLtb reports these parameters, together with the input P-T values that used for orthopyroxene-liquid and clinopyroxene-liquid thermobarometers, in a tabulated form between column numbers 1 and 203 in the *Calculation Screen* window. Clinopyroxene-, orthopyroxene-, liquid-clinopyroxene- and liquid-orthopyroxene-related parameters are highlighted by the light cyan, light green, faded pink and light yellow colors in the *Calculation Screen*, respectively.

All data in the *Calculation Screen* can be sent to a Microsoft® Excel file (i.e. Output.xlsx) by clicking the *Send Results to Excel* icon or selecting same option from the pull-down *Excel* menu. Similarly, an output Excel file can be displayed by clicking the *Open Excel file* option from the pull-down menu of *Excel*. WinPLtb is a compiled program that consists of a self-extracting setup file, including support files for the Microsoft® Visual Studio package not installed on the computer, help file, data files (e.g. pyx, xls, and xlsx), and Grapher plot document files (e.g. grf files). By clicking the setup file, the program and its associated files are installed into the directory of "C:\Program Files\WinPLtb" in the 32-bit system or "C:\Program Files (x86)\WinPLtb" in the 64-bit system. The self-extracting setup file is approximately 14 Mb and can be obtained from the journal server or from corresponding author on request.

ACKNOWLEDGEMENTS

We would like to thank Silvio Mollo and Cristina Perinelli for their noteworthy contributions and suggestions on manuscript and program code that improved the manuscript.

REFERENCES

Armienti P., Perinelli C., Putirka K.D., 2013. A new model to estimate deep-level magma ascent rates, with applications to Mt Etna (Sicily, Italy). Journal of Petrology 54, 795-813.

Beattie P., 1993. Olivine-melt and orthopyroxene-melt equilibria. Contributions to Mineralogy and Petrology 115, 103-111.

Blundy J., Cashman K., 2008. Petrologic reconstruction of magmatic system variables and processes. Minerals, Inclusions and Volcanic Processes: Reviews in Mineralogy & Geochemistry 69, 179-239.

DeBari S.M., Greene A.R., 2011. Vertical stratification of composition, density, and inferred magmatic processes in exposed arc crustal sections. In: Arc-Continental Collision, Frontiers in Earth Sciences. (Eds.): D. Brown and P.D. Ryan, Springer-Verlag, Berlin, 121-144.

Droop G.T.R., 1987. A general equation for estimating Fe^{3+} concentrations in ferromagnesian silicates and oxides from microprobe analyses, using stoichiometric criteria. Mineralogical Magazine 51, 431-435.

Edmonds M., Wallace P.J., 2017. Volatiles and exsolved vapor in volcanic systems. Elements 13, 29-34.

Gómez J.M.C., 1990. PX: a program for pyroxene classification and calculation of end-members. American Mineralogist 75, 1426-1427.

Harmon L.J., Crowlyn J., Gualda G.A.R., Ghiorso M.S., 2018. Phase-equilibrium geobarometers for silicic rocks based on rhyolite-MELTS. Part 4: plagioclase, orthopyroxene, clinopyroxene, glass geobarometer, and application to Mt. Ruapehu, New Zeland. Contributions to Mineralogy and Petrology 173, 7, 1-20.

Hill D.P. and Zucca J.J., 1987. Geophysical constraints on the structure of Kilauea and Mauna Loa volcanoes and some imlications for seismomagmatic processes. U.S. Geological Survey Professional Paper 1350, 903-917.

Hora J.M., Kronz A., Möller-McNett S., Wörner G., 2013. An Excel-based tool for evaluating and visualizing geothermobarometry data. Computers & Geosciences 56, 178-185.

Lanari P., Vidal O., Andrade V.D., Dubacq B., Lewin E., Grosch E.G., Schwartz S., 2014. XMapTools: A MATLAB©-based program for electron microprobe X-ray image processing and geothermobarometry. Computers & Geosciences 62, 227-240.

Lepage L.D., 2003. ILMAT: an Excel worksheet for ilmenite-magnetite geothermometry and geobarometry. Computers & Geosciences 29, 673-678.

Locock A.J., 2014. An Excel spreadsheet to classify chemical analyses of amphiboles following the IMA 2012 recommendations. Computers & Geosciences 62, 1-11.

Masotta M., Mollo S., Freda C., Gaeta M., Moore G., 2013. Clinopyroxene-liquid thermometers and barometers specific to alkaline differentiated magmas. Contributions to Mineralogy and Petrology 166, 1545-1561.

Mavko B.B., Thompson G.A., 1983. Crustal and upper mantle structure of the northern and central Sierra Nevada. Journal of Geophysical Research 88, 5874-5892.

McHone J.G., 1987. PXC: an APL program for calculating pyroxene structural formulae and end members. Computers & Geosciences 13, 89-91.

Mollo S., Gaeta M., Freda C., Di Rocco T., Misiti V., Scarlato P., 2010a. Carbonate assimilation in magmas: a reappraisal based on experimental petrology. Lithos 114, 503-514.

Mollo S., Del Gaudio P., Ventura G., Lezzi G., Scarlato P., 2010b. Dependence of clinopyroxene composition on cooling rate in basaltic magmas: implications for thermobarometry. Lithos 118, 302-312.

Neave D.A., Putirka K.D., 2017. A new clinopyroxene-liquid barometer, and implications for magma storage pressures under Icelandic rift zones. American Mineralogist 102, 777-794.

Nimis P., 1995. A clinopyroxene geobarometer for basaltic systems based on crystal-structure modeling. Contributions to Mineralogy and Petrolgy 121, 44-125.

Papike J.J., Cameron K.L., Baldwin K., 1974. Amphiboles and pyroxenes: characterization of other than quadrilateral components and estimates of ferric iron from microprobe data, Geological Society of America Abstract Program 6, 1053-1054.

Perinelli C., Mollo S., Gaeta M., Cristofaro S.P.D., Palladino D.M., Armienti P., Scarlato P., Putirka K.D., 2016. An improved clinopyroxene-based hygrometer for Etnean magmas and imlications for eruption triggering mechanisms. American Mineralogist 101, 2774-2777.

Prezzi C.B., Gotze H.-J., Schmidt S., 2009. 3D density model of the central Andes. Physics of the Earth and Planetary Interiors

177, 217-234.
Putirka K., 1997. Magma transport at Hawaii: inferences based on igneous thermobarometry. Geology 25, 69-72.
Putirka K., Johnson M., Kinzler R., Longhi J., Walker D., 1996. Thermobarometry of mafic igneous rocks based on clinopyroxene-liquid equilibria, 0-30 kbar. Contributions to Mineralogy and Petrology 123, 92-108.
Putirka K.D., Mikaelian H., Ryerson F., Shaw H., 2003. New clinopyroxene-liquid thermobarometers from mafic, evolved, and volatile-bearing lava compositions, with applications to lavas from Tibet and the Snake River Plain, Idaho. American Mineralogist 88, 1542-1554.
Putirka K.D., 2008. Thermometers and barometers for volcanic systems. Minerals, Inclusions and Volcanic Processes: Reviews in Mineralogy & Geochemistry 69, 61-120.
Putirka K.D., 2018a. Orthopyroxene-based Thermobarometers (Orthopyroxene.xls). http://www.fresnostate.edu/csm/ees/documents/facstaff/putirka/excel-sheets/Orthopyroxene.xls. (accessed 02.04.18).
Putirka K.D., 2018b. Clinopyroxene-based Thermobarometers (Clinopyroxene_P-T_9-26-16). http://www.fresnostate.edu/csm/ees/documents/Clinopyroxene_P-T_9-26-16.xlsx. (accessed 02.04.18).
Soto J.I. and Soto M.V., 1995. PTMAFIC: Software package for thermometry, barometry, and activity calculations in mafic rocks using IBM-compatible computer. Computers & Geosciences 21, 619-652.
Sturm R., 2002. PX-NOM- an interactive spreadsheet program for the computation of pyroxene analyses derived from the electron microprobe. Computers & Geosciences 28, 473-483.
Winter John D., 2001. An Introduction to Igneous and Metamorphic Petrology. Prentice Hall, New Jersey, 697 pp.
Yavuz F., 1998. BIOAPAG-PC: Program for an apatite and biotite geothermometer. Computers & Geosciences 24, 885-891.
Yavuz F., 1999. A revised program for microprobe-derived amphibole analyses using the IMA rules. Computers & Geosciences 25, 909-927.
Yavuz F., 2001. PYROX: A computer program for the IMA pyroxene classification and calculation scheme. Computers & Geosciences 27, 97-107.
Yavuz F., 2003a. Evaluating micas in petrologic and metallogenic aspect: I-definitions and structure of the computer program MICA+. Computers & Geosciences 29, 1203-1213.
Yavuz F., 2003b. Evaluating micas in petrologic and metallogenic aspect: II-Applications using the computer program MICA+. Computers & Geosciences 29, 1215-1228.
Yavuz F., 2007. WinAmphcal: a windows program for the IMA-04 amphibole classification. Geochemistry Geophysics Geosystems 8, Q01004. https://dx.doi.org/10.1029/2006GC001391.
Yavuz F., Yavuz V., Sasmaz A., 2006. WinClastour—a Visual Basic program for tourmaline formula calculation and classification. Computers & Geosciences 32, 1156-1168.
Yavuz F., 2013. WinPyrox: A Windows program for pyroxene calculation classification and thermobarometry. American Mineralogist 98, 1338-1359.
Yavuz F., Karakaya N., Yıldırım D.K., Karakaya M.Ç., Kumral M., 2014. A Windows program for calculation and classification of tourmaline-supergroup (IMA-2011). Computers & Geosciences 63, 70-87.
Yavuz F., Kumral M., Karakaya N., Karakaya M.Ç., Yıldırım D.K., 2015. A Windows program for chlorite calculation and classification. Computers & Geosciences 81, 101-113.
Yavuz F., Döner Z., 2017. WinAmptb: A Windows program for calcic amphibole thermobarometry. Periodico di Mineralogia 86, 135-167.

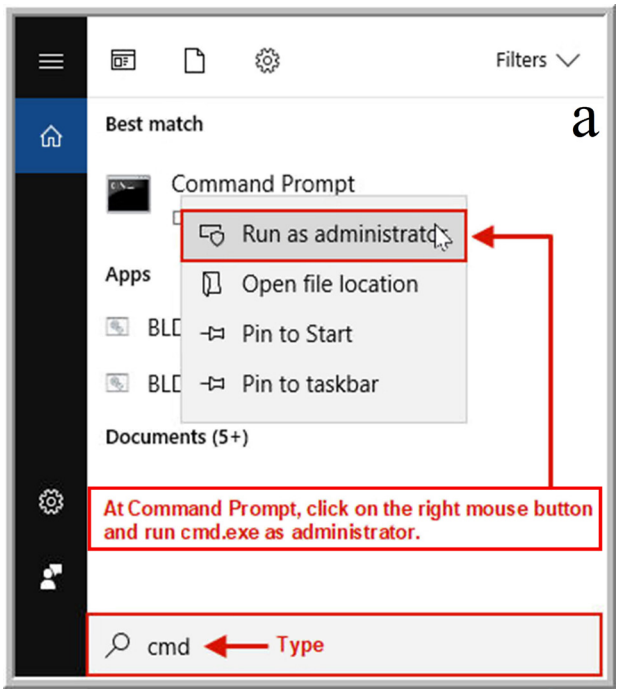

APPENDIX

WinPLtb runs properly in a personal computer with the 32-bit operating system. An execution of program in a personal computer with the 64-bit operating system, however requires the following steps by users for registration of the MSFLXGRD.OCX component.

i) Click the "Start" button and type cmd.exe in the search box (see Figure a).

ii) Run cmd.exe as administrator (see Figure a).

iii) Type regsvr32 /u "C:\Program Files (x86)\WinPltb\MSFLXGRD.OCX and press ENTER key (see Figure b).

iv) Type regsvr32 "C:\Program Files (x86)\WinPltb\MSFLXGRD.OCX and press ENTER key (see Figure b).

v) Click the WinPLtb icon on desktop to execute the program (see Figure b).

Figure a,b. Screen captures showing the registration of MSFLEXGRD.OCX component in a personal computer using Windows 10 with the 64-bit operating system.